

# *S*-Type and *P*-Type Habitability in Stellar Binary Systems: A Comprehensive Approach

## II. Elliptical Orbits

M. Cuntz

*Department of Physics*

*University of Texas at Arlington, Arlington, TX 76019-0059;*

cuntz@uta.edu

### ABSTRACT

In the first paper of this series, a comprehensive approach has been provided for the study of *S*-type and *P*-type habitable regions in stellar binary systems, which was, however, restricted to circular orbits of the stellar components. Fortunately, a modest modification of the method also allows for the consideration of elliptical orbits, which of course entails a much broader range of applicability. This augmented method is presented here, and numerous applications are conveyed. In alignment with Paper I, the selected approach considers a variety of aspects, which comprise the consideration of a joint constraint including orbital stability and a habitable region for a possible system planet through the stellar radiative energy fluxes (“radiative habitable zone”; RHZ). The devised method is based on a combined formalism for the assessment of both *S*-type and *P*-type habitability; in particular, mathematical criteria are deduced for which kinds of systems *S*-type and *P*-type habitable zones are realized. If the RHZs are truncated by the additional constraint of orbital stability, the notation of *ST*-type and *PT*-type habitability applies. In comparison to the circular case, it is found that in systems of higher eccentricity, the range of the RHZs is significantly reduced. Moreover, for a considerable number of models, the orbital stability constraint also reduces the range of *S*-type and *P*-type habitability. Nonetheless, *S*-, *P*-, *ST*-, and *PT*-type habitability is identified for a considerable set of system parameters. The method as presented is utilized for **BinHab**, an online code available at The University of Texas at Arlington.

*Subject headings:* astrobiology — binaries: general — celestial mechanics — planetary systems

## 1. INTRODUCTION

A major task situated at the crossroad of stellar astrophysics, also encompassing orbital stability studies and astrobiology, is the identification of habitable zones (HZs) of stars, including binaries and multi-stellar systems. Recent studies for those systems have been given by, e.g., Eggl et al. (2012), Kaltenegger & Haghighipour (2013a,b), Kane & Hinkel (2013), Kane et al. (2014), Cuntz (2014), Jaime et al. (2014), and Cuntz & Bruntz (2014). The fact that planets are able to exist in binary systems has been pointed out in numerous observational investigations and surveys, including Patience et al. (2002), Eggenberger et al. (2004); Eggenberger & Udry (2007), Raghavan et al. (2006, 2010), and Roell et al. (2012).

Earlier work also targeted planet formation in binary systems, including terrestrial planets, as summarized by Kley & Nelson (2012). That work contains a thorough review of our current understanding of disk–planet interactions, including prevalent processes of planet growth within gaseous protoplanetary disks, as well as the exchange of angular momentum between planets and the disk and planet migration. Important results have also been provided by the *Kepler* mission, which include the detection of planets in stellar binary systems. Examples include Kepler-16 (Slawson et al. 2011; Doyle et al. 2011), and Kepler-47 (Orosz et al. 2012). Kepler-16b constitutes the first circumbinary planet (*P*-type orbit), which means that it orbits both binary components. Theoretical simulations on the habitability of possible Earth-mass planets and moons in that system have been given by Quarles et al. (2012). Kepler-47, on the other hand, is host to at least three planets in orbit around both stars.

A previous study focused on *S*-type and *P*-type habitable zones in binary systems has been given by Cuntz (2014), henceforth called Paper I. The focus of this work was the study of habitable regions for systems with the stellar components in circular orbits, a limitation that will be overcome in the present work. Observationally, it is found that the stars residing in binary systems are almost always in elliptical orbits, with some systems exhibiting fairly high eccentricities; see, e.g., Roell et al. (2012) and references therein. Examples include  $\gamma$  Cep A ( $e_b = 0.41$ ), HD 196885 A ( $e_b = 0.42$ ), and HD 126614 A ( $e_b \leq 0.6$ ). In these systems, the planet is orbiting one of the stellar components (*S*-type orbit), with the other stellar component acting as a perturber. Also, there is high diversity regarding stellar component combinations. For the cases discussed by Roell et al. (2012) (see their Table 2), the primaries span between spectral types F, G, and K, whereas the secondaries are mostly M-type dwarfs.

Akin to the previous work of Paper I, numerous aspects have been taken into account, including: (1) the consideration of a joint constraint including orbital stability and a habitable region for a possible system planet through the stellar radiative energy fluxes (“radiative

habitable zone”; RHZ); (2) the treatment of conservative, general and extended zones of habitability for the various systems as defined for the Solar System and beyond (see Section 2.1); (3) the provision of a combined formalism for the assessment of both *S*-type and *P*-type habitability; in particular, mathematical criteria are presented for which kind of system *S*-type and *P*-type habitability is realized. Specifically, an algebraic formalism for the assessment of both *S*-type and *P*-type habitability is employed based on a fourth order polynomial. Thus, an a priori specification for the presence or absence of *S*-type or *P*-type RHZs is neither necessary nor possible, as those are determined by the adopted mathematical formalism.

In principle, five different cases of habitability are identified, which are: *S*-type and *P*-type habitability provided by the full extent of the RHZs; habitability, where the RHZs are truncated by the additional constraint of planetary orbital stability (referred to as *ST*- and *PT*-type, respectively); and cases of no habitability at all. On the other hand, Paper I solely focused on circular binary systems. Fortunately, a modest modification of the method forwarded by Paper I allows for the consideration of elliptical orbits, which provide a much broader range of applicability, including detailed comparisons with observations as well as a large realm of theoretical studies. Emphasis is placed again on the detailed calculations of the RHZs and the orbital stability criterion for theoretical planets, which again will utilize the previous work by Holman & Wiegert (1999), thereafter HW99.

Paper II is structured as follows: In Section 2, we describe the theoretical approach, particularly the adopted modifications to the circular case as studied in Paper I, which concern both the computation of the RHZs and the planetary orbital stability limits. In Section 3, we provide various case studies regarding *S*-, *ST*-, *P*-, and *PT*-type habitability. Special emphasis is placed on the width of stellar habitable zones as function of the binary eccentricity as well as the domains of the conservative and general zones of habitability for different sets of system parameters. Our summary and conclusions are given in Section 4.

## 2. THEORETICAL APPROACH

### 2.1. Calculation of the RHZs

In the following, we summarize the information needed for the calculations of the RHZs in binary systems regarding both *S*-type and *P*-type orbits. This effort deals with the requirement of providing a habitable region for a system planet based on the radiative energy fluxes of the stellar components. The requirement of orbital stability will be disregarded for now; it will be discussed in Section 2.2. The adopted approach is fairly similar to that of Paper I, which focused on binary systems in circular orbits. Akin to Paper I, we focus on

theoretical main-sequence stars (see Table 1). A flow diagram of the code, named **BinHab**, also described by Cuntz & Bruntz (2014), is given as Figure 1.

The key equations of the adopted method read as follows. For a star of luminosity  $L_i$  (in units of solar luminosity  $L_\odot$ ), the distance  $d_i$  of the habitability limit  $s_\ell$  as identified for the Sun (see Paper I and references therein), constituting either an inner or outer limit of a stellar habitable region (except for  $\ell = 3$ ; see Table 2), is given as

$$d_i = s_\ell \sqrt{\frac{L_i}{S_{\text{rel},i\ell} L_\odot}}. \quad (1)$$

Here  $S_{\text{rel},i\ell} = S_{\text{rel},i\ell}(T_{\text{eff}})$  describes the stellar flux in units of the solar constant, which is a function of the stellar effective temperature  $T_{\text{eff}}$  (e.g., Kasting et al. 1993, and subsequent work). The values for  $S_{\text{rel},i\ell}$  are calculated following the formalism of Selsis et al. (2007); see Paper I for additional information.

In the solar case, it is found that the conservative habitable zone (CHZ) extends between 0.95 and 1.37 AU (i.e.,  $\ell = 2$  and 4, respectively), and the general habitable zone (GHZ) extends between 0.84 and 1.67 AU (i.e.,  $\ell = 1$  and 5, respectively)<sup>1</sup>. Following Underwood et al. (2003) and references therein, the inner limit of the CHZ is defined by water loss, occurring when the atmosphere is warm enough to build a stratosphere where water is gradually lost by photodissociation and subsequent hydrogen loss to space. The outer limit of the CHZ is defined by first carbon dioxide condensation. Moreover, the GHZ is defined by the domain between the runaway greenhouse effect (inner limit) and the maximum greenhouse effect (outer limit). The extreme case of the extended habitable zone (EHZ), attained through excessive planetary global greenhouse processes, is in the solar case assumed to extend up to 2.40 AU (Forget & Pierrehumbert 1997; Mischna et al. 2000), i.e.,  $\ell = 6$ . Furthermore,  $\ell = 3$  is used for identifying Earth-equivalent positions, as done in Paper I.

In case of a binary system with planetary distances  $d_i$ , limits of habitability associated

---

<sup>1</sup>Recent studies indicate that setting those limits is a more complex process than adopted by Kasting et al. (1993) as they depend on, e.g., particulars of the planetary atmosphere (as manifested through detailed 3-D modeling), geodynamics, rotation rate, and mass; see, e.g., Von Bloh et al. (2009), Seager (2013), Leconte et al. (2013), Zsom et al. (2013), Kopparapu et al. (2013, 2014), and Yang et al. (2014), for details. Updated limits can thus be considered through interpolation between the results obtained for the inner / outer limits of the CHZ and GHZ. Alternatively, updates in the limits for the CHZ and GHZ can be considered through appropriate choices for  $s_\ell$  (see Table 2), as anticipated in the forthcoming version of **BinHab**.

with  $s_\ell$  are obtained through solving

$$\sum_{i=1}^2 \frac{L_i}{S_{\text{rel},i\ell} d_i^2} = \frac{L_\odot}{s_\ell^2}. \quad (2)$$

It is found that

$$d_1^2 = a^2 + z^2 + 2az \cos \varphi \quad (3a)$$

$$d_2^2 = a^2 + z^2 - 2az \cos \varphi. \quad (3b)$$

Here  $a \equiv a_b$  denotes the semi-distance of the binary components (or a modified value of it, see below, with  $a_b$  being used if the original denotation applies),  $z$  the distance of a position at the habitability limit contour, also referred to as radiative habitable limit (RHL), and  $\varphi$  the associated angle; see Figure 2 for information on the coordinate set-up for both  $S$ -type and  $P$ -type orbits. It is also assumed that  $L_1 \geq L_2$  without loss of generality. Following Paper I, we again introduce the concept of recast stellar luminosity  $L'_{i\ell}$  defined as

$$L'_{i\ell} = \frac{L_i}{L_\odot S_{\text{rel},i\ell}}. \quad (4)$$

Finally, following algebraic transformations, the equation for  $z(\varphi)$  is obtained as

$$z^4 + A_2 z^2 + A_1 z + A_0 = 0 \quad (5)$$

with

$$A_2 = 2a^2(1 - 2\cos^2 \varphi) - s_\ell^2(L'_{1\ell} + L'_{2\ell}) \quad (6a)$$

$$A_1 = 2as_\ell^2 \cos \varphi (L'_{1\ell} - L'_{2\ell}) \quad (6b)$$

$$A_0 = a^4 - a^2 s_\ell^2 (L'_{1\ell} + L'_{2\ell}). \quad (6c)$$

As discussed in Paper I, Equation (5) constitutes a fourth-order algebraic equation that is known to possess four possible solutions (Bronstein & Semendyayev 1997), although some (or all) of them may constitute unphysical solutions, i.e.,  $z(\varphi)$  having a complex or imaginary value. The solutions of this polynomial allow to define the inner and outer limits of the RHZs based on the system parameters. Equation (5) is solved using the adopted coordinate system, which in essence constitutes a polar coordinate system, except that negative values for  $z$  are permitted; in this case the position of  $z$  is found on the opposite side of angle  $\varphi$ . This approach allows to identify the various cases for the existence of solutions for  $z(\varphi)$  in regard to  $S$ -type and  $P$ -type habitable regions.

It is noteworthy that heretofore the method of solution as presented is identical to that for binary components in circular orbits. Thus, the decisive question arises as to how the

RHZs for binary components in elliptical orbits can adequately be addressed. In this regard, the underlying assumption of this study needs to be taken into account, which is that *any system planet deemed potentially habitable needs to be located within the system’s RHZ at all times*. This standard needs to be applied regardless of the (time-dependent) separation of the binary components, i.e., whether the system components are in a periastron  $a_{\text{per}}$ , apastron  $a_{\text{ap}}$ , or any intermediate position.

Consequently, the most stringent positioning for the inner and outer limits of the RHZs, taking into account all possible separations of the binary components, including the periastron and apastron positions, must be taken into account. This implies that both for  $S$ -type and  $P$ -type habitability, for any inner RHL, the outermost position must be selected, whereas for any outer RHL, the innermost position must be selected to define the annuli for the RHZs. Based on detailed analyses, exemplified by Figure 3 and 4 (see discussion below), as well as results given in Section 3, encompassing both equal-mass and nonequal-mass binary systems, it is found that for  $S$ -type RHZs, regarding inner RHLs, the periastron stellar positions need to be chosen, i.e.,  $a_{\text{b}}(1 - e_{\text{b}})$ , whereas regarding outer RHLs, the apastron stellar positions need to be chosen, i.e.,  $a_{\text{b}}(1 + e_{\text{b}})$ . However, for  $P$ -type RHZs, both regarding the inner and outer RHLs, the apastron positions need to be chosen throughout (see Table 2).

Algebraically, it is found that for  $P$ -type orbits, the extrema  $\text{RHZ}_{\text{in}}$  and  $\text{RHZ}_{\text{out}}$  are given as

$$\text{RHZ}_{\text{in}} = \text{Max}(\mathcal{R}(z, \varphi)) \Big|_{s_{\ell, \text{in}}} \Big|_{a=a_{\text{ap}}} \quad (7a)$$

$$\text{RHZ}_{\text{out}} = \text{Min}(\mathcal{R}(z, \varphi)) \Big|_{s_{\ell, \text{out}}} \Big|_{a=a_{\text{ap}}}, \quad (7b)$$

whereas for  $S$ -type orbits, the extrema  $\text{RHZ}_{\text{in}}$  and  $\text{RHZ}_{\text{out}}$  are given as

$$\text{RHZ}_{\text{in}} = \text{Max}(\mathcal{R}(z, \alpha)) \Big|_{s_{\ell, \text{in}}} \Big|_{a=a_{\text{per}}} \quad (8a)$$

$$\text{RHZ}_{\text{out}} = \text{Min}(\mathcal{R}(z, \alpha)) \Big|_{s_{\ell, \text{out}}} \Big|_{a=a_{\text{ap}}}, \quad (8b)$$

respectively, noting that  $\mathcal{R}(z, \alpha)$  and  $\mathcal{R}(z, \varphi)$  describe the areas bordered by the RHLs defined by  $s_{\ell, \text{in}}$  and  $s_{\ell, \text{out}}$  (see Paper I). The calculation of the extrema is applied to the angles  $\alpha$  ( $S$ -type systems) and  $\varphi$  ( $P$ -type systems) for the intervals  $0 \leq \alpha \leq \pi$  and  $0 \leq \varphi \leq \pi/2$ , respectively. For  $P$ -type systems, the coordinate information is provided by Figure 2. Note that for  $S$ -type systems, the angle’s fix point is at the stellar primary S1.

The necessity for the choices  $a = a_{\text{per}}$  or  $a = a_{\text{ap}}$  is illustrated by the following instructive examples (conveyed in high precision for tutorial reasons), which refer to equal-mass binary systems with  $M_1 = M_2 = M_{\odot}$  for an eccentricity of  $e_{\text{b}} = 0.30$  (see Figure 3), and with

the RHLs inspected for the GHZ. As a first case, we consider a system assuming a major axis of  $2a_b = 1.0$  AU; in this case, the RHZ is given as *P*-type. At the periastron position for the system components, the inner and outer limits for the RHLs are given as 1.436 and 2.567 AU, respectively. However, at the system’s apastron position, the inner and outer limits for the RHLs are given as 1.663 and 2.508 AU, respectively. Intermediate values for the inner and outer limits of the RHLs are obtained for other positions of the system, as expected. Therefore, the most stringent inner and outer limits for the overall RHZ annulus are identified as 1.663 and 2.508 AU, which are the values for the system’s apastron position.

As a second case, we study a system with a major axis of  $2a_b = 20.0$  AU; in this case, the RHZ is given as *S*-type (see Figure 4). At the system’s periastron position, the inner and outer limits for the RHLs concerning the GHZ are identified as 0.9300 and 1.8443 AU, respectively. Furthermore, at the system’s apastron position, the inner and outer limits for the RHLs are identified as 0.9283 and 1.8359 AU, respectively, with intermediate values for the inner and outer limits of the RHLs obtained for other positions. Thus, the most stringent inner and outer limits for the overall RHZ annulus are identified as 0.9300 and 1.8359 AU. In this case, the relevant value for the inner RHL is given by the system’s periastron position, whereas relevant value for outer RHL is given by the system’s apastron position. Note that the same kind of behavior is identified for other sets of system parameters, such as stellar masses (including binary systems of unequal masses), major axes  $2a_b$ , and eccentricities  $e_b$ . It also holds for the different types of HZs, i.e., CHZs, GHZs, and EHZs.

Thus, in terms of the derivations obtained in Paper I, all equations still hold, except that  $a$  needs to be replaced by  $a \mapsto \tilde{a}_{SP,\ell}$ , where  $\tilde{a}_{SP,\ell}$  must be set as either  $a_b(1 - e_b)$  or  $a_b(1 + e_b)$ , depending on the selection of  $\ell$  and whether *S*-type or *P*-type RHZs are considered (see Table 2). Hence, the entire previously given mathematical evaluations, including the transformations for general binary systems represented through a fourth-order polynomial, continue to hold as virtually all equations<sup>2</sup> and analyses are distinctly separate for inner and outer RHLs; this feature applies to both equal-mass and non-equal mass binary systems.

One decisive connection between inner and outer RHLs is given by the requirement that for a *P*-type habitable region, the inner RHL  $s_{\ell,\text{in}}$  must be located completely inside the outer RHL  $s_{\ell,\text{out}}$  for the corresponding RHZ to exist, i.e.,

$$\text{Min}\left(\mathcal{R}(z, \varphi)\right)\Big|_{s_{\ell,\text{out}}} \geq \text{Max}\left(\mathcal{R}(z, \varphi)\right)\Big|_{s_{\ell,\text{in}}}, \quad (9)$$

where  $\mathcal{R}(z, \varphi)$  denotes the domain bordered by the respective RHLs. As noted in Paper I,

---

<sup>2</sup>The exception is Equation (45) of Paper I, which however can be replaced by the more general Equation (40) of Paper I.

this condition is, however, violated in some models, especially for relatively large values of  $a$ , as well as relatively small ratios of  $L'_{2\ell}/L'_{1\ell}$ . In this case, the RHZ for  $(s_{\ell,\text{in}}, s_{\ell,\text{out}})$  is nullified, a behavior that may occur for the pairings  $(s_2, s_4)$ ,  $(s_1, s_5)$ , and  $(s_1, s_6)$ , corresponding to the CHZ, GHZ, and EHZ, respectively.

## 2.2. The Planetary Orbital Stability Constraint

As noted in previous investigations, habitability in multi-stellar systems (including binaries) requires—among other aspects—planetary orbital stability. In earlier work, Dvorak (1986) identified upper and lower bounds of planetary orbital stability considering the orbital elements, semimajor axis and eccentricity of the adopted binary stars. Within the last thirty years, a large body of additional studies has been performed encompassing both numerical and analytical work. Recent examples for the restricted three-body problem, but also containing assessments about general cases, have been given by Musielak & Quarles (2014). Previously, HW99 derived fitting formulae of orbital stability limits for both  $S$ -type and  $P$ -type planets in binary systems given as

$$\frac{a_{\text{cr}}}{a_{\text{b}}} = \sum_{i=0}^2 \tilde{A}_i \mu^i + \mathcal{F}_{\text{S}}(\mu, e_{\text{b}}) \quad (10)$$

and

$$\frac{a_{\text{cr}}}{a_{\text{b}}} = \sum_{i=0}^2 \tilde{A}_i \mu^i + \mathcal{F}_{\text{P}}(\mu, e_{\text{b}}), \quad (11)$$

respectively.

These equations communicate the critical semimajor axis  $a_{\text{cr}}$  in units of the semimajor axis  $a$  in the cases of  $S$ -type and  $P$ -type orbits. For  $S$ -type orbits, the ratio  $a_{\text{cr}}/a_{\text{b}}$ , see Equation (10), conveys the *upper limit* of planetary orbital stability, whereas for  $P$ -type orbits, the ratio  $a_{\text{cr}}/a_{\text{b}}$ , see Equation (11), conveys the *lower limit* of planetary orbital stability. Here  $\mu$  denotes the stellar mass ratio, given as  $\mu = M_2/(M_1 + M_2)$ , where  $M_1$  and  $M_2$  describe the two masses of the binary components with  $M_2 \leq M_1$ . The above given equations also include the parameter functions  $\mathcal{F}_{\text{S}}(\mu, e_{\text{b}})$  and  $\mathcal{F}_{\text{P}}(\mu, e_{\text{b}})$ , which depend on the mass ratio  $\mu$  and the eccentricity of the stellar binary,  $e_{\text{b}}$ , and are non-zero for elliptical binary systems<sup>3</sup>.

---

<sup>3</sup>In Paper I, we only included the linear term of  $\mu$  for the sake of parallelism between the treatment of  $S$ -type and  $P$ -type orbits.



Following HW99,  $\mathcal{F}_S$  and  $\mathcal{F}_P$  are given as

$$\mathcal{F}_S = e_b \sum_{i=0}^2 \tilde{B}_i \mu^i + e_b^2 \sum_{i=0}^2 \tilde{C}_i \mu^i \quad (12)$$

and

$$\mathcal{F}_P = e_b \sum_{i=0}^2 \tilde{B}_i \mu^i + e_b^2 \sum_{i=0}^2 \tilde{C}_i \mu^i, \quad (13)$$

respectively (see Table 3 for details). Equations (12) and (13) constitute second-order polynomial fits on results of orbital stability simulations by HW99 and previous work. The underlying studies explore the survival times of theoretical planets, treated as test particles, in various binary systems. Furthermore, based on HW99’s work, the Equations (10) to (13) are invalid for eccentricities beyond 0.8. Therefore, we limit the scope of the present study to binary systems with eccentricities in the range of  $0.0 \leq e_b \leq 0.80$ .

### 2.3. General Impact of the Binary System Eccentricity

Next we discuss the general impact of the eccentricity of a binary system on the different types of habitability, which can best be understood by comparing cases of relatively high eccentricity to the circular case (i.e.,  $e_b = 0$ ). First, we consider the impact of the binary system eccentricity on the RHZs. Examples are given in Figure 5, which depicts systems of stellar masses of  $M_1 = M_2 = M_\odot$ , as well as of  $M_1 = 1.5 M_\odot$  and  $M_2 = 0.5 M_\odot$ , taking the GHZ as test cases. (The aspect that nonequal-mass binary systems compared to equal-mass binary systems, with  $M_1 + M_2$  kept constant, have largely reduced RHZs, albeit  $L_1 + L_2$  of the nonequal-mass system is notably higher due to the mass–luminosity relationship, has been one of the main foci of Paper I.) The major axis is assumed as  $2a_b = 1.0$  AU; furthermore, we consider binary eccentricities of  $e_b = 0.0$  and  $0.5$ . In case of equal masses and  $e_b = 0.0$  the inner and outer RHLs are given as 1.54 and 2.54 AU, respectively. For  $e_b = 0.5$ , however, the inner and outer RHLs are given as 1.75 and 2.11 AU, respectively. Thus, if  $e_b$  is increased, the inner RHL moves outward, whereas the outer RHL moves inward. Therefore, the total width of the RHZ is reduced from 1.0 AU to 0.36 AU.

An even more dramatic reduction of the RHZ occurs for unequal mass systems. Taking  $M_1 = 1.5 M_\odot$  and  $M_2 = 0.5 M_\odot$  as an example, it is found that for  $e_b = 0$ , the inner and outer RHLs are given as 2.16 and 2.66 AU, respectively. For  $e_b = 0.5$ , the inner and outer RHLs are given as 2.41 and 2.45 AU, respectively. In this case, the RHZ is virtually nonexistent; its width has been reduced by 91% relative to the circular case, whereas in the equal-mass system previously discussed, the reduction is “only” 64%. Note that reductions

in the RHZs also occur for  $S$ -type habitable regions. However, for those models, the effects of increased values for  $e_b$  are very small, or minuscule, as verified by numerous case studies (see Section 3.3). For the above-given examples of  $M_1$  and  $M_2$  with  $2a_b = 20$  AU, the RHZs are marginally reduced both for the equal and non-equal mass system, noting that the reduction relative to the circular case are given as 0.8% and 0.04%, respectively.

Another important aspect concerns the influence of  $e_b$  on the orbital stability behavior of possible planets. Generally, it is found that if  $e_b$  is increased, the domain of stability is reduced both for  $S$ -type and  $P$ -type orbits. If  $e_b$  is larger than zero, the orbital stability limit for  $P$ -type orbits (which constitutes a lower limit) is positioned further outward, whereas for  $S$ -type orbits, the orbital stability limit (which constitutes an upper limit) is positioned further inward. Evidently, both types of behavior affect the domains of planetary orbital stability in an adverse manner. To showcase this type of behavior, we evaluated both  $\mathcal{F}_P$  and  $\mathcal{F}_S$  for different values of  $e_b$ , given as 0.0, 0.3, and 0.5. For  $\mu = 0.25$ ,  $\mathcal{F}_P$  is identified as 2.31, 3.35, and 3.85, respectively, corresponding to an increase by a factor of 1.67. For  $\mu = 0.50$ ,  $\mathcal{F}_P$  is identified as 2.39, 3.18, and 3.60, respectively, corresponding to an increase by a factor of 1.5. It is found that the orbital stability limit moves outward if  $e_b$  is increased, thus reducing the width of the RHZ (if any) compatible with planetary orbital stability. For  $S$ -type habitability, the following results are found. For  $\mu = 0.25$ ,  $\mathcal{F}_S$  is obtained as 0.369, 0.233, and 0.152, and for  $\mu = 0.50$ ,  $\mathcal{F}_S$  is obtained as 0.274, 0.177, and 0.118, respectively, for the sequence of  $e_b = 0.0, 0.3, \text{ and } 0.5$  (see above). Hence, for  $\mu = 0.25$  and 0.50,  $\mathcal{F}_S$  is reduced by a factor of about 2.4 if  $e_b$  is raised from 0.0 to 0.5. As for  $S$ -type orbits, the planetary orbital stability limit constitutes an upper limit, which is found to be placed further inward for systems of higher binary eccentricity; thus, the width of the RHZ (if any) compatible with planetary orbital stability is reduced as well.

In summary, increased values of eccentricity in binary systems entail an adverse impact both regarding  $P$ -type and  $S$ -type habitability, due to their influence both on the widths of the RHZs (if any) and on the domains of stability for possible circumbinary or circumstellar planets.

### 3. RESULTS AND DISCUSSION

#### 3.1. Examples of $S$ -, $ST$ -, $P$ -, and $PT$ -type Habitability Solution Domains

In the following, we study examples of  $S$ -,  $ST$ -,  $P$ -, and  $PT$ -type habitability aimed at highlighting the impact of binary eccentricity. Our study comprises an equal-mass system of  $M_1 = M_2 = 1.0 M_\odot$  with a luminosity of  $L_1 = L_2 = 1.23 L_\odot$  (see Figure 6) and a nonequal-

mass system of  $M_1 = 1.25 M_\odot$  and  $M_2 = 0.75 M_\odot$  (see Figure 7); here the luminosities are given as  $L_1 = 2.15 L_\odot$  and  $L_2 = 0.36 L_\odot$ . The habitable regions are calculated for the GHZ. The overall approach is to place the two stellar components at different separation distances, i.e., with the major axis  $2a_b$  considered the independent variable, and to assess resulting domains of habitability. The systems are evaluated for fixed values of binary eccentricity, given as  $e_b = 0.0, 0.25, 0.5,$  and  $0.75$ .

Regarding  $P$ -type orbits, it is found that increased values of binary eccentricity affect the widths of the RHZs as well as the maximum value of the major axis  $2a_b$ , for which  $P$ -type RHZs can exist. This type of behavior is found for both the equal-mass and the nonequal-mass system. For the equal-mass binary system, the width of the RHZ at 0.05 AU (a distance where also the orbital stability criterion is readily met) is given as 1.20, 1.16, 1.11, and 1.06 AU for models of  $e_b = 0.0, 0.25, 0.5,$  and  $0.75$ , respectively. For the nonequal-mass binary system, the width of the RHZ at 0.05 AU is identified as 0.91, 0.82, 0.74, and 0.67 AU, respectively. These results show that higher values of  $e_b$  entail smaller widths of the RHZ and that for given values of  $e_b$ , the width of the RHZ is noticeably smaller in the nonequal-mass system than in the equal-mass system, even though the latter has a higher combined stellar luminosity ( $L_1 + L_2$ ).

Regarding the orbital stability limit, which for  $P$ -type orbits constitutes a lower limit (see Section 2.2), the following behavior is found: If the major axis of the stellar components is increased, the limit moves inward. Therefore, the stellar separation distance must be relatively small for the full width of the RHZ to be available for  $P$ -type habitability. For models of increased values of  $e_b$ , the requirement of stellar proximity becomes more rigorous; in the depiction of Figures 6 and 7, this more-stringent requirement corresponds to a larger slope of the orbital stability cut-off line. In the eight examples given in Figures 6 and 7, there are also domains of  $PT$ -type habitability, i.e., where some, but not all, of the  $P$ -type RHZ is available for circumbinary habitability; however, they are relatively small, if not minuscule.

$S$ -type RHZs are also influenced by the eccentricity of the binary system, though the effects are relatively minor. For binary systems with a major axis of  $2a_b = 15$  AU, the following behavior occurs. For the equal-mass system of Figure 6,  $\text{RHZ}_{\text{in}}$  changes from 0.930 to 0.985 AU, and  $\text{RHZ}_{\text{out}}$  changes from 1.843 to 1.836 AU if the system's eccentricity is increased from 0.0 to 0.75. Furthermore, for the nonequal-mass system,  $\text{RHZ}_{\text{in}}$  changes from 1.209 to 1.234 AU, and  $\text{RHZ}_{\text{out}}$  changes from 2.341 to 2.338 AU if the system's eccentricity is increased from 0.0 to 0.75. Hence, the width of the RHZ for the equal-mass system decreases from 0.91 to 0.85 AU, whereas the width of the RHZ for the nonequal-mass system decreases from 1.13 to 1.10 AU between the circular case and  $e_b = 0.75$ . Thus, increased values of eccentricity reduce the width of the RHZs for  $S$ -type systems as well. However, it is also

found that the width of the RHZ in the nonequal-mass binary system is consistently higher than in the equal-mass binary system owing to the influence of  $L_1$ .

Regarding the orbital stability limit, which for  $S$ -type orbits constitutes an upper limit (see Section 2.2), the following behavior is identified: If the major axis of the stellar components is increased, the orbital stability limit moves outward. Therefore, the stellar separation distance must be relatively large for the full width of the RHZ to be available for  $S$ -type habitability. For models of increased values of  $e_b$ , the requirement of a sufficiently large stellar separation distance is highly rigorous;  $S$ -type habitability is only available for relatively large  $2a_b$  values. In Figures 6 and 7, the more-stringent requirement of orbital stability for larger values of  $e_b$  amounts to a decrease in the slope of the orbital stability cut-off line.

The effect of the system’s eccentricity on its ability to provide  $S$ -type habitable regions is remarkable. For  $e_b$  of 0.0, 0.25, 0.5, and 0.75,  $S$ -type habitability occurs at minimum major axes of 13.5, 19.1, 31.1, and 74.5 AU, respectively, for the equal-mass system (see Figure 6) and at 14.8, 21.2, 35.1, and 84.9 AU, respectively, for the nonequal-mass system (see Figure 7). Higher values of the system’s eccentricity also imply larger domains of  $ST$ -type habitability. If  $e_b$  is increased from 0.0 to 0.5 or 0.75, the domains of  $ST$ -type habitability change from 6.6 to 15.2 or 36.5 AU for the equal-mass system and from 7.2 to 16.9 or 41.0 AU for the nonequal-mass system. The reason for this pattern is that in systems of high eccentricity, the stars are in relatively close proximity at their periastron positions, which adversely affects both the  $S$ -type and  $ST$ -type habitable regions due to the orbital stability requirement. Considering major axes of  $2a_b = 15$  AU for the four equal-mass systems as well as the four nonequal-mass systems studied in detail,  $S$ -type and  $ST$ -type habitability are found for one system each, whereas the case of no habitable region is encountered for two systems each.

In summary, it is found that increased values of binary eccentricity affect the RHZs (though the change in  $S$ -type RHZs is very minor) and pose a highly unfavorable impact on the domains of orbital stability of possible system planets. These findings apply to both  $S$ -type and  $P$ -type habitability. Additional case studies for  $S$ -type and  $P$ -type systems are given in Section 3.3 and 3.2, respectively. Our focus will be systems of different combinations of  $M_1$  and  $M_2$  and, by implication,  $L_1$  and  $L_2$ , to evaluate the zones of circumstellar and circumbinary habitability.

### 3.2. Case Studies of $P/PT$ -type Habitability

In the following, we present case studies pertaining to  $P/PT$ -type habitability. Owing to the many possible sets of parameter combinations, encompassing the stellar major axis  $2a_b$ , the binary eccentricity  $e_b$ , and the stellar masses  $M_1$  and  $M_2$ , it will not be feasible to provide a fully comprehensive analysis. However, it will be possible to focus on various cases, selected for tutorial purposes, by using  $2a_b = 0.5, 0.75, \text{ and } 1.0$  AU. Moreover, some intriguing aspects will be targeted such as (1) the study of main-sequence stars of different masses, i.e., between  $1.25$  and  $0.50 M_\odot$ , (2) the extent and position of the RHZs in the various models, as well as the impact of the planetary orbital stability requirement, and (3) the critical value of  $e_b$ , below which—depending on the model— $P/PT$ -type habitable regions are able to exist.

Akin to Paper I, we concentrate on systems of main-sequence stars; see Table 1 for information on the stellar parameters. One of our goals is to inspect the values for  $\text{RHZ}_{\text{in}}$  and  $\text{RHZ}_{\text{out}}$  at the stellar periastron and apastron position, i.e.,  $a_{\text{per}}$  and  $a_{\text{ap}}$ , respectively, to obtain additional data to justify the method adopted for calculating the RHZs (see Section 2.1). We also include systems of low-mass / low-luminosity stars, corresponding to stellar types K and M, which is motivated by their relatively high abundance (i.e., up to about 90%), owing to the skewness of the Galactic initial mass function (e.g., Kroupa 2001, 2002; Chabrier 2003). Our results are depicted in Table 4 to 8.

Table 4 and 5 convey results for equal-mass binary systems of  $M_1 = M_2 = 1.0 M_\odot$  regarding both the CHZ and GHZ, respectively, for  $2a_b = 0.5, 0.75, \text{ and } 1.0$  AU for different eccentricities of the binary components. Data are given for both the RHZ (see column “Orbit”) and the orbital stability limited denoted as  $a_{\text{cr}}$ . It is found that for both the CHZ and GHZ, the  $\text{RHZ}_{\text{in}}$  and  $\text{RHZ}_{\text{out}}$  significantly depend on the system’s eccentricity  $e_b$  with  $2a_b$  assumed to be fixed. Specifically,  $\text{RHZ}_{\text{in}}$  increases and  $\text{RHZ}_{\text{out}}$  decreases as functions of  $e_b$ . Hence, for any system with a prescribed value for  $2a_b$ , the RHZs narrow if  $e_b$  is increased.

For the CHZ (Table 4), the width of the RHZ between  $e_b = 0.0$  and  $0.8$  changes from  $0.56$  to  $0.41$  AU in systems of  $2a_b = 0.50$  AU and from  $0.48$  to  $0.18$  in systems of  $2a_b = 0.75$  AU. For  $2a_b = 1.0$  AU, the width of the RHZ for  $e_b = 0.0$  is given as  $0.36$  AU; however, no RHZ is found beyond  $e_b = 0.64$ , owing to the fact that the inner and outer RHL intersect. The planetary orbital stability limit  $a_{\text{cr}}$ , constituting a lower limit for circumbinary habitability, is relatively small. Therefore, if the CHZ-RHZs exist, which occurs for most values of  $e_b$ ,  $P$ -type habitable regions are realized. For the GHZ (Table 5), the width of the RHZ between  $e_b = 0.0$  and  $0.8$  changes from  $1.20$  to  $1.05$  AU in systems of  $2a_b = 0.50$  AU, from  $1.11$  to  $0.82$  AU in systems of  $2a_b = 0.75$  AU, and from  $1.00$  to  $0.39$  AU in systems of  $2a_b = 1.0$  AU. As expected, in all of these models, the GHZ is consistently wider than the CHZ. Moreover,

$P$ -type habitability is identified in all models, except beyond  $e_b = 0.41$  for  $2a_b = 1.0$  AU, where  $PT$ -type habitability occurs. For  $e_b = 0.8$  and  $2a_b = 1.0$  AU, the width of the RHZ is given as 0.55 AU, whereas the width of the  $PT$ -type HZ is given as 0.39 AU due to truncation.

Table 6 and 7 convey results for nonequal-mass binary systems of  $M_1 = 1.25 M_\odot$  and  $M_2 = 0.75 M_\odot$ . We again focus on both the CHZ and GHZ for  $2a_b = 0.5, 0.75,$  and  $1.0$  AU for different eccentricities of the binary components. Again, regarding both the CHZ and the GHZ, respectively, the  $\text{RHZ}_{\text{in}}$  and  $\text{RHZ}_{\text{out}}$  significantly depend on  $e_b$ ; i.e.,  $\text{RHZ}_{\text{in}}$  increases and  $\text{RHZ}_{\text{out}}$  decreases as a function of  $e_b$ , entailing that the RHZs narrow with increasing values of  $e_b$ . This feature has profound consequences for our models; particularly, for  $2a_b = 0.75$  AU, no habitable regions exist for systems of  $e_b > 0.29$  pertaining to the CHZ. Moreover, no habitable regions exist for systems of  $2a_b = 1.0$  AU regardless of the eccentricity of the binary components, including systems with the stars in circular orbits.

Regarding the GHZ, a different type of picture emerges. Here,  $P$ -type habitability is identified for the nonequal-mass system previously studied, irrespective of  $e_b$ . However, the  $P$ -type HZ critically narrows as a function of  $e_b$ . The width of the RHZ between  $e_b = 0.0$  and  $0.8$  changes from 0.91 to 0.66 AU in systems of  $2a_b = 0.50$  AU, from 0.74 to 0.38 AU in systems of  $2a_b = 0.75$  AU, and from 0.60 to 0.09 AU in systems of  $2a_b = 1.0$  AU. Furthermore, owing to the orbital stability limit, which constitutes a lower limit, the kind of habitability identified is  $P$ -type rather than  $PT$ -type. Comparing our findings for the nonequal-mass binary system to the results obtained for the equal-mass binary system indicates that circumbinary habitable regions (if existing) are much narrower in nonequal-mass compared to equal-mass systems, a result in alignment with the discussion of Section 2.3.

Another approach to demonstrate the impact of the binary eccentricity  $e_b$  on the domains of  $P/PT$ -type habitability is to evaluate the quantities  $\% \text{RHZ}$  and  $\% \text{HZ}$  for the various models.  $\% \text{RHZ}$  denotes the relative size of the RHZ for a given set of models with the special case of  $e_b = 0$  set as 100 (see Tables 4 to 7). Moreover,  $\% \text{HZ}$  denotes relative size of the HZ. In the absence of restrictions due to the orbital stability constraint,  $\% \text{RHZ}$  and  $\% \text{HZ}$  are identical; otherwise,  $\% \text{HZ}$  is smaller than  $\% \text{RHZ}$ . For a distinct type of model, defined by a given value of  $2a_b$ , the choice of CHZ or GHZ (with the EHZ disregarded in the following), and the stellar masses  $M_1$  and  $M_2$ , it is found that both  $\% \text{RHZ}$  and  $\% \text{HZ}$  decrease with increasing values for  $e_b$ .

The results provided by the Tables 4 to 7 allow us to assess for which type of models the decrease in  $\% \text{RHZ}$  and  $\% \text{HZ}$  for increasing values of  $e_b$  is most severe. In conclusion, it is found that the decrease is most severe for relatively large values of  $2a_b$ , if the CHZ considered instead of the GHZ, and for unequal-mass systems compared to equal-mass systems if  $(M_1 + M_2)$  remained unaltered. With  $e_b = 0.5$  taken as an instructive example, the results of our

models read as follows: For the CHZ and regarding  $2a_b = 0.5, 0.75,$  and  $1.0$  AU, %RHZ is given as 85, 64, and 24, respectively. Furthermore, there is also no difference between %RHZ and %HZ, as for those models the habitable regions are consistently identified as  $P$ -type. Regarding the GHZ, %RHZ is identified as 93, 84, and 73, respectively. However, the model for  $2a_b = 1.0$  AU is identified as  $PT$ -type; hence, %HZ is found as 68, which is smaller than %RHZ.

Additionally, we focus on the results for nonequal-mass binary systems of  $M_1 = 1.25 M_\odot$  and  $M_2 = 0.75 M_\odot$ . With  $e_b = 0.5$  again used as an example, we obtained the following results. For the CHZ and for  $2a_b = 0.5$  AU, %RHZ is given as 45. However, there are no solutions for either  $2a_b = 0.75$  or  $1.0$  AU. For the latter case, there is even no solution for circular systems defined through  $e_b = 0.0$ . For the GHZ, the results read as follows: Regarding  $2a_b = 0.5, 0.75,$  and  $1.0$  AU, %RHZ is given as 82, 70, and 49, respectively. %RHZ follows the same trend previously identified. Regarding the GHZ, there is also no difference between the values for the %RHZ and the %HZ, as the habitable regions are identified as  $P$ -type.

Table 8 lists the results for  $e_b$  (crit.), defined as the maximum value of  $e_b$  for a given system, classified by  $2a_b, M_1,$  and  $M_2,$  for which a habitable region can still be identified. Note that  $e_b$  (crit.) has been evaluated in increments of 0.01, except when it was identified as below 0.01. In this case, increments of 0.001 were used. Regarding  $P/PT$ -type systems, the absence of habitable regions is either due to the intersect between  $RHL_{in}$  and  $RHL_{out}$  (see Equation 9), or because the planetary orbital stability requirement is violated. Table 8 shows that for most systems of  $2a_b = 0.5$  AU studied, the choice of  $e_b$  presents little hindrance for the occurrence of circumbinary HZs. Exceptions include, however, some cases of low-mass stellar systems, especially systems of  $M_2 = 0.50 M_\odot$ . If the GHZ is assumed instead of the CHZ, the number of cases without  $P/PT$ -type habitability is further reduced. For the majority of models studied with major axes of 0.5 AU, it is found that  $0.8 \leq e_b(\text{crit.}) < 1$ . Furthermore, for models with major axes of 1.0 AU,  $e_b$  (crit.) is often identified as relatively small, or, alternatively, circumbinary habitability is absent altogether. Especially if the CHZ is considered rather than the GHZ, circumbinary habitability is highly restricted. The only exception is the case of  $M_1 = M_2 = 1.25 M_\odot$ , where in the framework of our model no restriction for  $e_b$  has been identified.

Figure 8 provides a summary of  $P/PT$ -type habitability for several equal-mass and nonequal-mass binary systems by displaying the widths of the respective HZs. It is found that for  $2a_b = 0.5$  AU, the impact of  $e_b$  on the size of the circumbinary HZs is not very large for most systems. However,  $2a_b = 1.0$  AU, the situation is notably different, also taking into account that for many cases circumbinary HZs can be found, especially for cases of

intermediate or high values of  $e_b$ . Moreover, Figure 8 also displays the widths of the EHZ for a selected number of cases. Here it is found that in many cases, the extent of the EHZ exceeds that for the GHZ by about a factor of 2, irrespective of the value adopted for  $e_b$ .

### 3.3. Case Studies of $S/ST$ -type Habitability

In the following, we describe results pertaining to  $S$ -type and  $ST$ -type habitability. Akin to Section 3.2, we again consider systems of main-sequence stars; see Table 1 for information on the stellar parameters. We also inspect the values for  $\text{RHZ}_{\text{in}}$  and  $\text{RHZ}_{\text{out}}$  at the stellar periastron and apastron position, denoted as  $a_{\text{per}}$  and  $a_{\text{ap}}$ , respectively, to provide additional verification for the method of calculating the RHZs for  $e_b > 0$  (see Section 2.1). Particularly, we include systems of low-mass / low-luminosity stars owing to their relatively high abundance; see Table 9 to 11 for a depiction of our results. Additional studies, including systems with binary masses of  $0.65 M_{\odot}$ , were given by Cuntz & Bruntz (2014). These studies are based on the same rigor and limitations as considered in Paper I and II.

Table 9 conveys results for equal-mass binary systems of  $M_1 = M_2 = 1.0 M_{\odot}$  regarding both the CHZ and GHZ for  $2a_b = 20$  AU for different eccentricities of the binary components. Information is given regarding both the RHZ (see column “Orbit”) and the orbital stability limited denoted as  $a_{\text{cr}}$ . It is found that regarding both the CHZ and GHZ, the  $\text{RHZ}_{\text{in}}$  and  $\text{RHZ}_{\text{out}}$  are only very weakly dependent on  $e_b$  except for cases beyond  $e_b \simeq 0.65$ , which are however of little interest because those cases lack habitability due to the orbital stability requirement. Thus, generally, the RHZs extend from 1.05 to 1.50 AU for the CHZ and from 0.93 to 1.84 AU for the GHZ. The orbital stability limit, which constitutes an upper limit, moves inward as a function of the binary eccentricity, starting at 2.74 AU for the circular case and taking values of 1.77 and 0.90 AU at  $e_b = 0.30$  and  $0.60$ , respectively. Therefore, for the CHZ,  $S$ -type habitability is obtained at eccentricities below 0.39, and  $ST$ -type habitability is obtained at eccentricities below 0.54; the latter value is again referred to as critical value of  $e_b$  (see also Table 11). Moreover, for the GHZ,  $S$ -type and  $ST$ -type habitability occurs below eccentricities of 0.28 and 0.59, respectively.

Table 10 conveys results for nonequal-mass binary systems of  $M_1 = 1.25 M_{\odot}$  and  $M_2 = 0.75 M_{\odot}$ . It is again found that for both the CHZ and GHZ, the  $\text{RHZ}_{\text{in}}$  and  $\text{RHZ}_{\text{out}}$  are barely dependent on  $e_b$  except for cases beyond  $e_b \simeq 0.65$ , which again are of little interest because they lack habitability due to the orbital stability requirement. It is found that the RHZs extend from 1.37 to 1.90 AU for the CHZ and from 1.21 to 2.34 AU for the GHZ. The orbital stability limit, which constitutes an upper limit, moves inward as a function of the binary eccentricity, starting at 3.22 AU for the circular case and taking values of 2.02 and



1.01 AU at  $e_b = 0.30$  and  $0.60$ , respectively. Compared to the previous case of the equal-mass binary system, both the RHZ-CHZ and the RHZ-GHZ are broader and are at a larger stellar distance due to the higher value of  $L_1$ , i.e.,  $2.15 L_\odot$  versus  $1.23 L_\odot$ . For the CHZ of the nonequal-mass system,  $S$ -type habitability is identified at eccentricities below  $0.33$ , and  $ST$ -type habitability is obtained at eccentricities up to  $0.49$ . Furthermore, for the GHZ,  $S$ -type and  $ST$ -type habitability exists up to eccentricities of  $0.21$  and  $0.54$ , respectively.

Figure 9 depicts the widths of  $S/ST$ -type habitable zones for the GHZ of various binary systems for  $2a_b = 15.0$  AU and  $2a_b = 20.0$  AU for various types of systems between masses of  $1.25 M_\odot$  and  $0.50 M_\odot$ . For some of the systems, information is also given regarding the CHZ and EHZ. The finding for the various models is that between the circular case of  $e_b = 0$  up to a distinct value of  $e_b$ , the widths of the HZs are constant ( $S$ -type habitability); thereafter, they decrease linearly as a function of  $e_b$  ( $ST$ -type habitability). Finally, for each model, the critical value of  $e_b$  is found. Beyond that value, no habitable region exists. Figure 9 and Table 11 allow for the identification of general properties of systems with different combinations of masses and, by implication, luminosities of the stellar components. The findings include that in models of low eccentricity, i.e.,  $e_b \simeq 0$ , the widths of the HZs are largely determined by the luminosity of the stellar primary, which means that the higher its luminosity the larger is the resulting HZ. This result is valid for the CHZ, GHZ, as well as the EHZ. In the absence of truncation imposed by the orbital stability limit, the widths for the EHZs are largest and the widths for the GHZs and CHZs are respectively smaller, as expected.

The width of the  $S$ -type habitable region is largest for systems where the stellar primary possesses the greatest luminosity. However, these systems are also characterized by relatively low critical values of  $e_b$  owing to highly efficient truncation of the RHZ due to the orbital stability limit because of the primary’s relatively high mass. Conversely, for systems of low luminosity, relatively high numbers for the critical value of  $e_b$  are obtained. Even though the  $S/ST$ -type habitable zones have small widths in most of those systems, habitability is still possible for systems of high eccentricity. For example, for systems of  $M_1 = 1.25 M_\odot$  and  $M_2 = 0.75 M_\odot$  with  $2a_b = 20$  AU, the critical values for the eccentricity of the binary components are given as  $0.49$  and  $0.54$  for the CHZ and GHZ, respectively. However, for systems of  $M_1 = M_2 = 0.75 M_\odot$ , the critical values of  $e_b$  are given as  $0.72$  and  $0.74$ , respectively. Moreover, for equal-mass systems of  $0.50 M_\odot$ , the critical values of  $e_b$  are larger than  $0.80$ , which is the upper limit for  $e_b$  considered in our study; see Table 11 and the work of Cuntz & Bruntz (2014) for additional results.

For  $2a_b = 20$  AU, we again studied the domains of the quantities %RHZ and %HZ for the various models. %RHZ denotes the relative size of the RHZ for a given set of

models with the special case of  $e_b = 0$  set as 100 (see Tables 9 to 10). Furthermore, %HZ denotes the relative size of the HZ, which contrary to the %RHZ also takes into account the orbital stability constraint; see Section 3.2 for results on the  $P/PT$ -type habitable regions. According to the model calculations-as-pursued, it was found that the decrease in the %RHZ for increasing values of  $e_b$  is very small. Regarding the 18 models for the equal-mass binary of  $M_1 = M_2 = 1.0 M_\odot$ , obtained with respect to the CHZ and GHZ, it is found that for 10 models, the reduction in the RHZ is less than 1%, and for 14 models, it is less than 2%. Nevertheless, for relatively high values of  $e_b$ , the reduction in the %HZ is highly notable due to the impact of the orbital stability constraint.

Regarding the 18 models for the nonequal-mass binary system given as  $M_1 = 1.25 M_\odot$  and  $M_2 = 0.75 M_\odot$ , the following behavior was identified. Here the reduction of the RHZ is even less significant than in the equal-mass system previously discussed. In fact, regarding the 18 models considered, the RHZ is reduced by 1% or less in 15 models, and by 2% or less in 17 models. This result is due to the the lower luminosity of the secondary star compared to the previous system. However, the impact of the orbital stability constraint in the nonequal-mass system is much more severe than in the equal-mass system previously discussed, as communicated by the numerical values of %HZ. Regarding the CHZ and GHZ, habitable regions are rendered impossible for eccentricities beyond 0.49 and 0.54, respectively (see Table 11).

Finally, we also compared systems of different major axes, specifically  $2a_b = 15$  AU and  $2a_b = 20$  AU. It was found that the widths of the HZs, especially for models of low eccentricity, were largely unaffected by the value of binary major axis; however, the critical values of  $e_b$  were still influenced by the choice of the major axis. These results are also consistent with the analysis of Figures 6 and 7 (see Section 3.1), which consider systems of different major axes  $2a_b$ . In those systems, the  $S$ -type RHZs were found to be largely independent of the values of the major axes; however, in systems of high eccentricity, habitability has been highly restricted or nullified due to the planetary orbital stability requirement.

#### 4. SUMMARY AND CONCLUSIONS

The method as described allows the calculation of  $S$ -type and  $P$ -type habitable zones in stellar binary systems.  $P$ -type orbits occur when the planet orbits both binary components, whereas in the case of  $S$ -type orbits, the planet orbits only one of the binary components with the second component considered a perturber. The selected approach considers a variety of aspects including: (1) besides simple cases, the treatment of nonequal-mass systems and systems in elliptical orbits; this latter aspect is a significant augmentation of the methodology

given in Paper I; (2) the consideration of a joint constraint, including orbital stability and a habitable region for a possible system planet through the stellar radiative energy fluxes; (3) the provision of a combined formalism for the assessment of both *S*-type and *P*-type habitability; in particular, through the solution of a fourth-order polynomial, mathematical criteria are employed for the kind of system in which *S*-type and *P*-type habitability is realized, an approach in alignment with that of Paper I.

If the RHZs are truncated by the additional constraint of orbital stability, the notation of *ST*-type and *PT*-type habitability is used. In comparison to the circular case, it is found that in systems of higher eccentricity, the domains of the RHZs are significantly reduced. Furthermore, the orbital stability constraint also impacts *S*-type and *P*-type habitability, in an unfavorable manner; this latter aspect is particularly relevant to the overall context of astrobiology. Nonetheless, *S*-, *P*-, *ST*-, and *PT*-type habitability is identified for a considerable set of system parameters. Compared to Paper I, which was focused on the circular case, a modest modification of the method allows for the consideration of elliptical orbits, entailing a significantly augmented range of applicability for the proposed method.

It is beyond the scope of this work to present a comprehensive parameter study. Besides the choice of the appropriate type of HZ, the system parameters for standard main-sequence stars (see Table 1) pertaining to our model include the major axis  $2a_b$ , the eccentricity of the binary components  $e_b$ , and the stellar luminosities  $L_1$  and  $L_2$ , or alternatively, the stellar masses  $M_1$ , and  $M_2$ . In the case of general stars, include subgiants and giants, the set of parameters would be further enlarged due to the lack of a universal mass–luminosity relationship. Selected results for low-mass main-sequence star binary systems have previously been given by Cuntz & Bruntz (2014).

It is found that an increased value for the eccentricity in stellar binary systems results in an adverse influence both regarding the RHZs and the orbital stability of possible system planets. For the latter, it is found that for *P*-type habitability, the limits of orbital stability move inward, and for *S*-type habitability, the limits of orbital stability move outward, thus potentially reducing the size of habitable regions for, respectively, circumbinary and circumstellar planets. Restrictions due to the orbital stability criterion are especially significant for *S*-type habitability for systems in highly elliptical orbits, since at the periastron position large segments of the RHZs are nullified. However, restrictions due to limited orbital stability in systems of highly elliptical orbits are less relevant regarding *P*-type habitability; in this case the most influential factor is given by the distribution of luminosity between the stellar components. As discussed in Paper I, highly unequal distributions of luminosity often entail small or nonexistent RHZs.

Our studies also show that increased eccentricities for the stellar binary components

lead to smaller widths of the HZs, as well as the lack of existence of HZs for relatively large values of  $e_b$ . In order to nonetheless offer some degree of habitability for systems in notably eccentric orbits, the finding places extra weight on previous studies, which show that under distinct conditions (e.g., relatively thick planetary atmospheres, distinct types of planetary atmospheric compositions) exoplanets are able to leave the RHZs without forfeiting habitability. For example, Williams & Pollard (2002) argued—based on 3-D general-circulation climate models and 1-D energy balance models aimed at examining Earth-type planets on extremely elliptical orbits near the HZ—exoplanets, as well as exomoons hosted by Jupiter-type planets (e.g., Heller 2012; Heller et al. 2014), will be able to harbor life even when undergoing excursions beyond the HZ. The reason is that in the framework of their models, long-term climate stability depends primarily on the average stellar flux received over an entire orbit, rather than the length of time spent within the HZ.

As previously discussed, a second criterion—besides the existence of the RHZs—for facilitating habitability consists in the orbital stability requirement. This criterion has heightened relevance compared to the radiative criterion because evidently “there is no way of escaping gravity” as due to system conditions, gravity-imposed planetary orbital instabilities may occur. Our present study employs the stability limits given by Holman & Wiegert (1999). They are based on numerical simulations for test particles able to survive  $10^4$  binary orbits. Considering the need for detailed habitability studies based on timescales of up to several billions of years, as implied by terrestrial biology, it appears appropriate to update the previous work of Holman & Wiegert based on significantly elongated timescales. An expected outcome of this type of investigation will be updated stability limits for both  $P$ -type and  $S$ -type orbits, which will likely be more stringent than currently attained.

Based on existing studies and tools given in the literature, future studies should include: (1) how limits of habitability (i.e.,  $s_\ell$ ; see Section 2.1) depend on the properties of the planet itself, such as planetary atmosphere, geodynamics, rotation rate, and mass; see, e.g., Von Bloh et al. (2009), Seager (2013), Leconte et al. (2013), Zsom et al. (2013), Kopparapu et al. (2013, 2014), and Yang et al. (2014), (2) models of binary systems where the component undergoes significant time-dependent evolution, and (3) models where the orbit of the terrestrial planet is misaligned with the orbital plane of the stellar binary components. This latter aspect is motivated by ongoing discoveries, including the detection of misaligned protoplanetary disks in the young binary system HK Tauri (Jensen & Akeson 2014). In this case, it is found that the disks are misaligned by  $60^\circ$  to  $68^\circ$ , such that one or both of the disks are significantly inclined to the binary orbital plane. Any future system planet will thus most likely result in a highly eccentric as well as inclined orbit. Such outcomes will pose a serious challenge to the calculation of both RHZs and orbital stability limits needed for future investigation of  $S$ - and  $P$ -type habitability.

This work has been supported in part by NASA’s Goddard Space Flight Center. The author acknowledges comments by Robert Bruntz and Billy Quarles as well as assistance by Satoko Sato and Zhaopeng Wang with computer graphics. He also wishes to draw the reader’s attention to the online code **BinHab**, hosted at The University of Texas at Arlington (UTA), which allows the calculation of habitable regions in binary systems based on the developed method.

## REFERENCES

- Bronshstein, I. N., & Semendyayev, K. A. 1997, *Handbook of Mathematics*, 3rd edn. (New York: Springer)
- Chabrier, G. 2003, *PASP*, 115, 763
- Chauvin, G., Beust, H., Lagrange, A.-M., & Eggenberger, A. 2011, *A&A*, 528, A8
- Cuntz, M. 2014, *ApJ*, 780, A14 [Paper I]
- Cuntz, M., & Bruntz, R. 2014, in *Cool Stars, Stellar Systems, and the Sun: 18th Cambridge Workshop*, ed. G. van Belle & H. Harris (Flagstaff: Proc. Lowell Observatory), in press (arXiv:1409.3449)
- Doyle, L. R., Carter, J. A., Fabrycky, D. C., et al. 2011, *Science*, 333, 1602
- Dvorak, R. 1986, *A&A*, 167, 379
- Eggenberger, A., Udry, S., & Mayor, M. 2004, *A&A*, 417, 353
- Eggenberger, A., & Udry, S. 2007, in *Planets in Binary Star Systems*, ed. Haghighipour (New York: Springer), p. 19
- Eggl, S., Pilat-Lohinger, E., Georgakarakos, N., Gyergyovits, M., & Funk, B. 2012, *ApJ*, 752, A74
- Forget, F., & Pierrehumbert, R. T. 1997, *Science*, 278, 1273
- Güdel, M., Dvorak, R., Erkaev, N., et al. 2014 in *Protostars and Planets VI*, in press (arXiv:1407.8174)
- Heller, R. 2012, *A&A*, 545, L8
- Heller, R., Williams, D., Kipping, D., et al. 2014, *Astrobiology*, in press (arXiv:1408.6164)
- Holman, M. J., & Wiegert, P. A. 1999, *AJ*, 117, 621 [HW99]
- Jaime, L. G., Aguilar, L., & Pichardo, B. 2014, *MNRAS*, 443, 260
- Jensen, E. L. N., & Akeson, R. 2014, *Nature*, 511, 567
- Kaltenegger, L., & Haghighipour, N. 2013a, *ApJ*, 777, A165
- Kaltenegger, L., & Haghighipour, N. 2013b, *ApJ*, 777, A166

- Kane, S. R., & Hinkel, N. R. 2013, *ApJ*, 762, A7
- Kane, S. R., Howell, S. B., Horch, E. P., et al. 2014, *ApJ*, 785, A93
- Kasting, J. F., Whitmire, D. P., & Reynolds, R. T. 1993, *Icarus*, 101, 108
- Kley, W., & Nelson, R. P. 2012, *ARA&A*, 50, 211
- Kopparapu, R. K., Ramirez, R., Kasting, J. F., et al. 2013, *ApJ*, 770, 82
- Kopparapu, R. K., Ramirez, R. M., Schottel Kotte, J., Kasting, J. F., Domagal-Goldman, S., & Eymet, V. 2014, *ApJ*, 787, L29
- Kroupa, P. 2001, *MNRAS*, 322, 231
- Kroupa, P. 2002, *Science*, 295, 82
- Lecante, J., Forget, F., Charnay, B., Wordsworth, R., Selsis, F., Millour, E., & Spiga, A. 2013, *A&A*, 554, A69
- Mischna, M. A., Kasting, J. F., Pavlov, A., & Freedman, R. 2000, *Icarus*, 145, 546
- Musielak, Z. E., & Quarles, B. 2014, *Rep. Prog. Phys.*, 77, 065901
- Orosz, J. A., Welsh, W. F., Carter, J. A., et al. 2012, *Science*, 337, 1511
- Patience, J., White, R. J., Ghez, A. M., et al. 2002, *ApJ*, 581, 654
- Quarles, B., Musielak, Z. E., & Cuntz, M. 2012, *ApJ*, 750, A14
- Raghavan, D., Henry, T. J., Mason, B. D., et al. 2006, *ApJ*, 646, 523
- Raghavan, D., McAlister, H. A., Henry, T. J., et al. 2010, *ApJS*, 190, 1
- Roell, T., Neuhäuser, R., Seifahrt, A., & Mugrauer, M. 2012, *A&A*, 542, A92
- Seager, S. 2013, *Science*, 340, 577
- Slawson, R. W., Prša, A., Welsh, W. F., et al. 2011, *AJ*, 142, 160
- Selsis, F., Kasting, J. F., Levrard, B., Paillet, J., Ribas, I., & Delfosse, X. 2007, *A&A*, 476, 1373
- Underwood, D. R., Jones, B. W., & Sleep, P. N. 2003, *Int. J. Astrobiol.*, 2, 289

Von Bloh, W., Cuntz, M., Schröder, K.-P., Bounama, C., & Franck, S. 2009, *Astrobiology*, 9, 593

Williams, D. M., & Pollard, D. 2002, *Int. J. Astrobiol.*, 1, 61

Yang, J., Boué, G., Fabrycky, D. C., & Abbot, D. S. 2014, *ApJ*, 787, L2

Zsom, A., Seager, S., de Wit, J., & Stamenković, V. 2013, *ApJ*, 778, A109



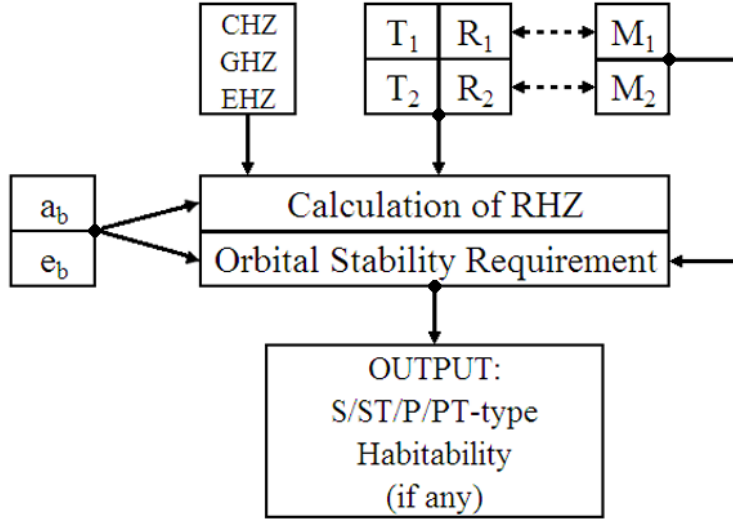


Fig. 1.— Flow diagram of **BinHab** indicating the adopted method of solution. Feed-ins and the generation of the output are indicated by arrowed solid lines. For theoretical main-sequence stars, effective temperatures and stellar radii ( $T_i$ ,  $R_i$ , with  $i = 1, 2$ ), on the one hand, or stellar masses ( $M_i$ ), on the other hand, may serve as input parameters, as indicated by double-arrowed dashed lines. See Cuntz & Bruntz (2014) for additional information.

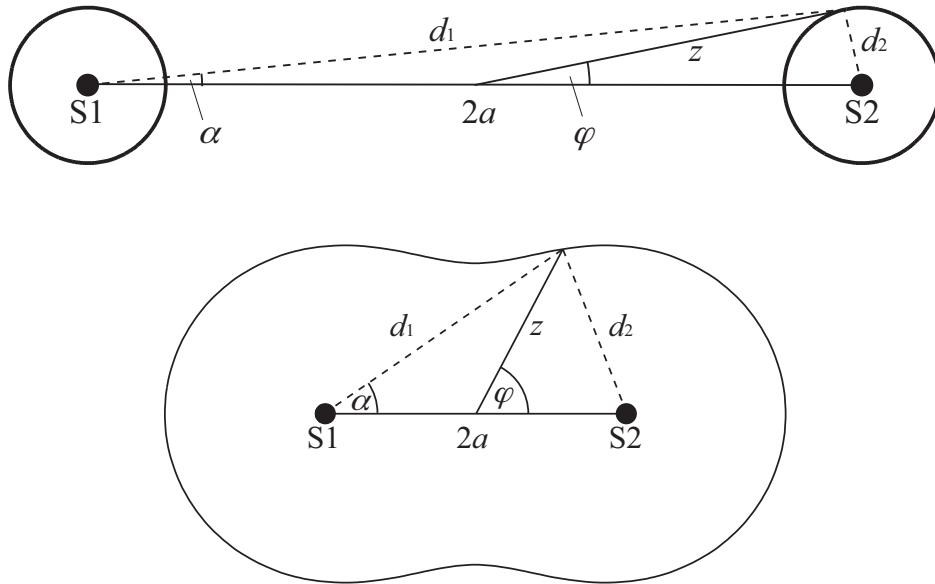


Fig. 2.— Set-up for the mathematical treatment of *S*-type (top) and *P*-type (bottom) habitable zones of binary systems as given by the stellar radiative fluxes with  $a \equiv a_b$ . Note that the stars S1 and S2 have been depicted as identical for convenience. (Adopted from Paper I.)

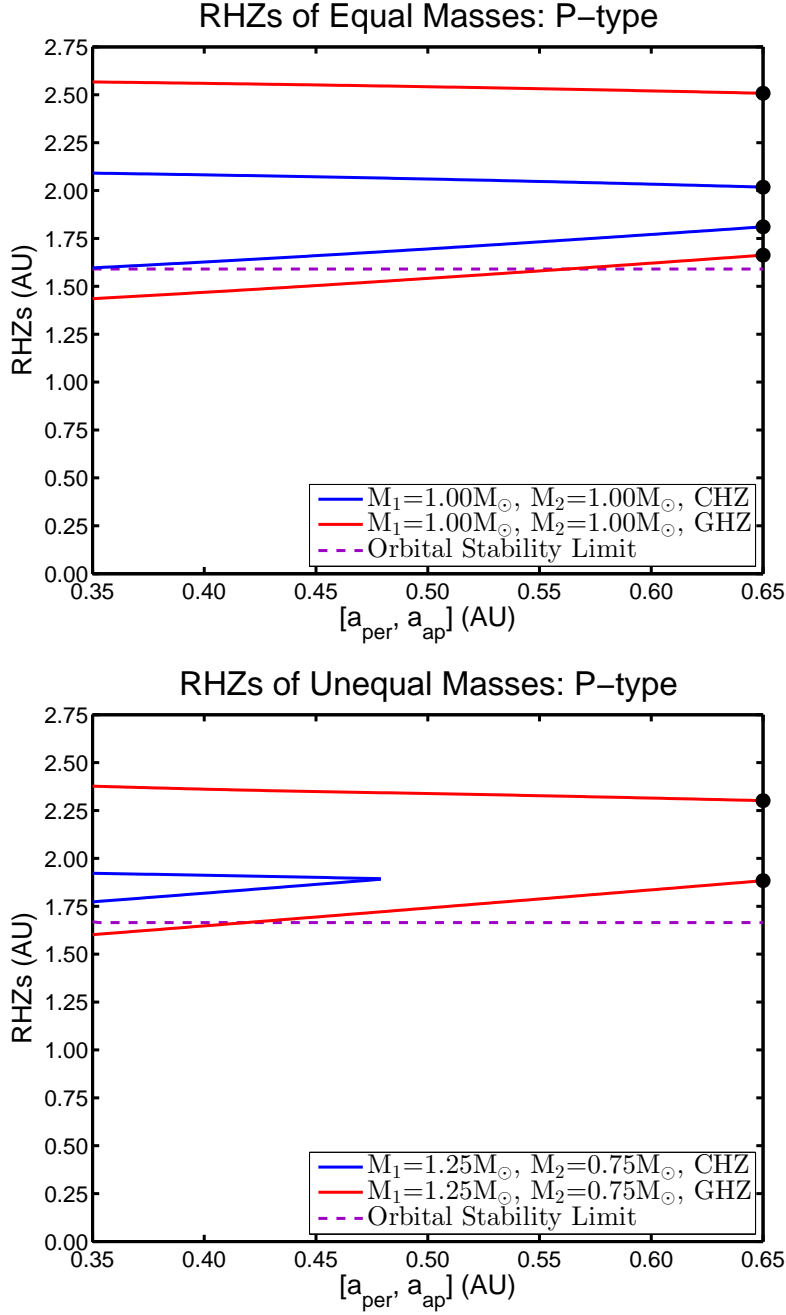


Fig. 3.— RHLs for  $P$ -type habitability for various models in the situations when the binary components are in periastron ( $a_{\text{per}}$ ), apastron ( $a_{\text{ap}}$ ), or intermediate position. The top panel depicts the case of  $M_1 = M_2 = M_\odot$ , whereas the bottom panel depicts the case of  $M_1 = 1.25 M_\odot$  and  $M_2 = 0.75 M_\odot$ . The models are for  $2a_b = 1.0$  AU and  $e_b = 0.30$ . The blue and red lines refer to the CHZ and GHZ, respectively. The planetary orbital stability limits are given as dashed purple lines for comparison. Note that both for the inner and outer limits of the RHZs, the apastron positions are decisive; therefore, they are indicated by black dots. Also, in case of the CHZ for unequal masses, no orbit-wide RHZ exists.

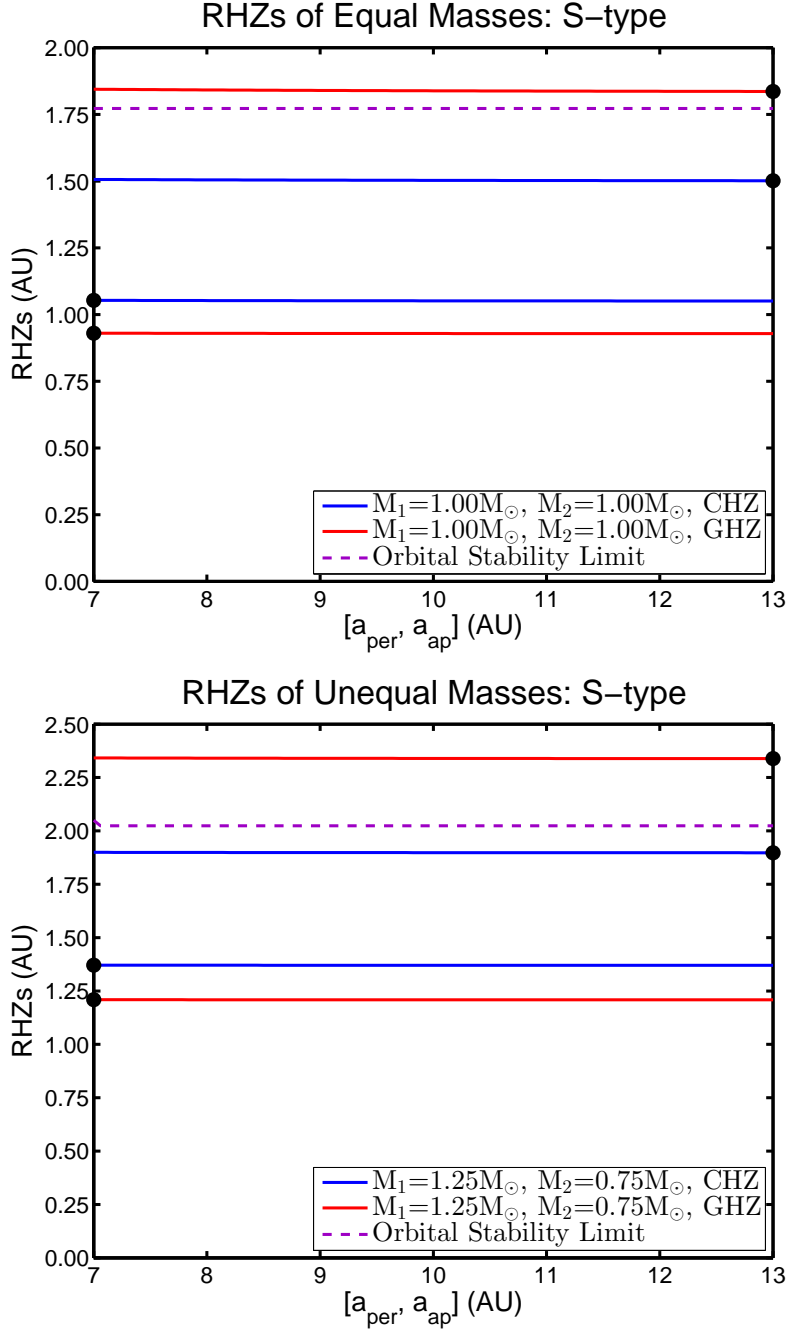


Fig. 4.— Same as Figure 3, but now regarding the RHLs for *S*-type habitability. The models are for  $2a_b = 20.0$  AU and  $e_b = 0.30$ . The red and blue lines refer to the GHZ and CHZ, respectively. The planetary orbital stability limits are given as dashed purple lines for comparison. Note that in case of *S*-type habitable regions, inner limits of the RHZs are set at the stellar periastron positions, whereas the outer limits of the RHZs are set at the stellar apastron positions. However, the differences for the RHLs between the  $a_{\text{per}}$  and  $a_{\text{ap}}$  positions are very minor.

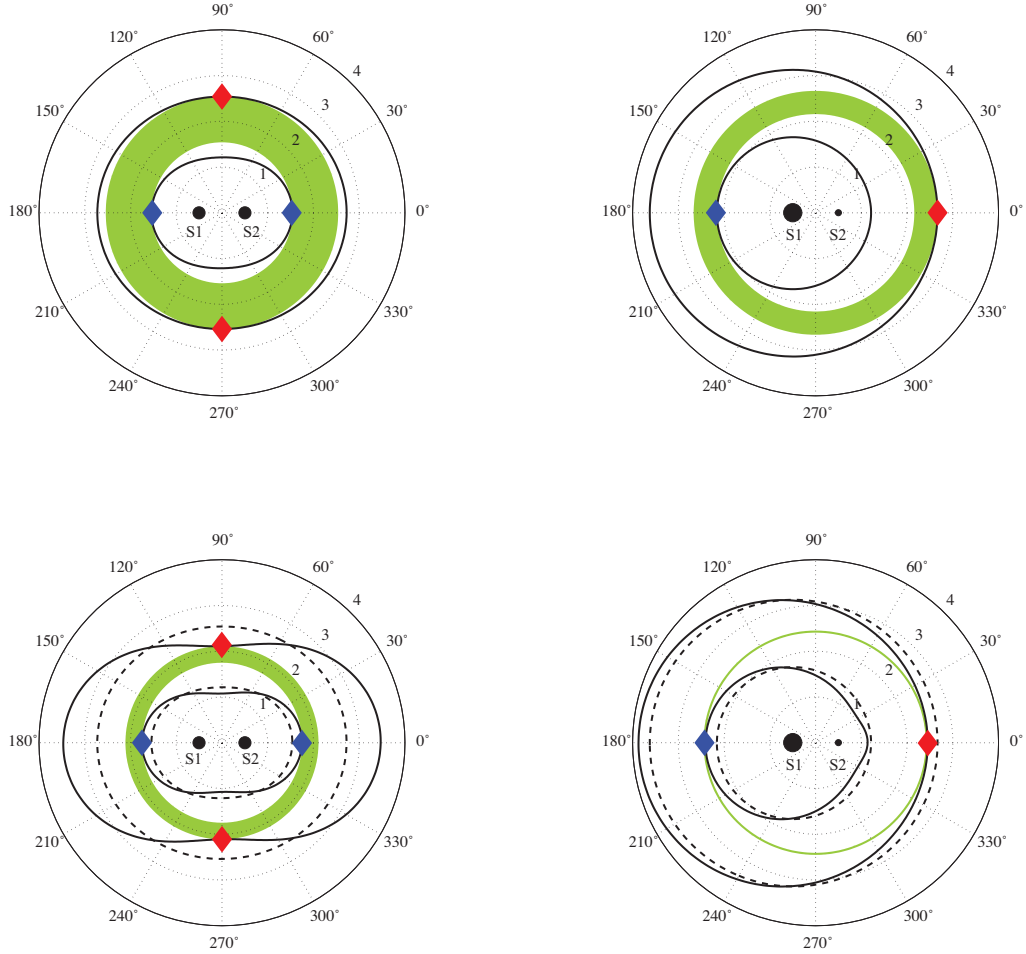


Fig. 5.— Examples of  $P$ -type RHZs for different systems. The solutions are given in polar coordinates, with the radial coordinate depicted in units of AU. The thick solid lines indicate the RHLs corresponding to the inner and outer limit of habitability, based on  $s_\ell = 0.84$  and  $1.67$  AU, respectively. The top row displays systems with  $e_b = 0.0$ , whereas the bottom row displays systems with eccentricity  $e_b = 0.5$ . Furthermore, there are different cases of stellar mass, and by implication stellar luminosity, noting that the left column features systems with  $M_1 = M_2 = M_\odot$ , whereas the right column features systems with  $M_1 = 1.5 M_\odot$  and  $M_2 = 0.5 M_\odot$ . The green areas indicate the appropriate circular regions (annuli), referred to as RHZs, for each case. The touching points between the RHZs and the inner and outer RHLs (utilized for the definition of the RHZs) are depicted as blue and red diamonds, respectively. For the elliptical systems (bottom row), the RHLs of the corresponding circular systems (top row) are given for comparison as dashed lines. Note that the extent of the RHZ is significantly reduced in systems of unequal stellar luminosities or nonzero eccentricity of the stellar components, with the most extreme reductions occurring for combined conditions.

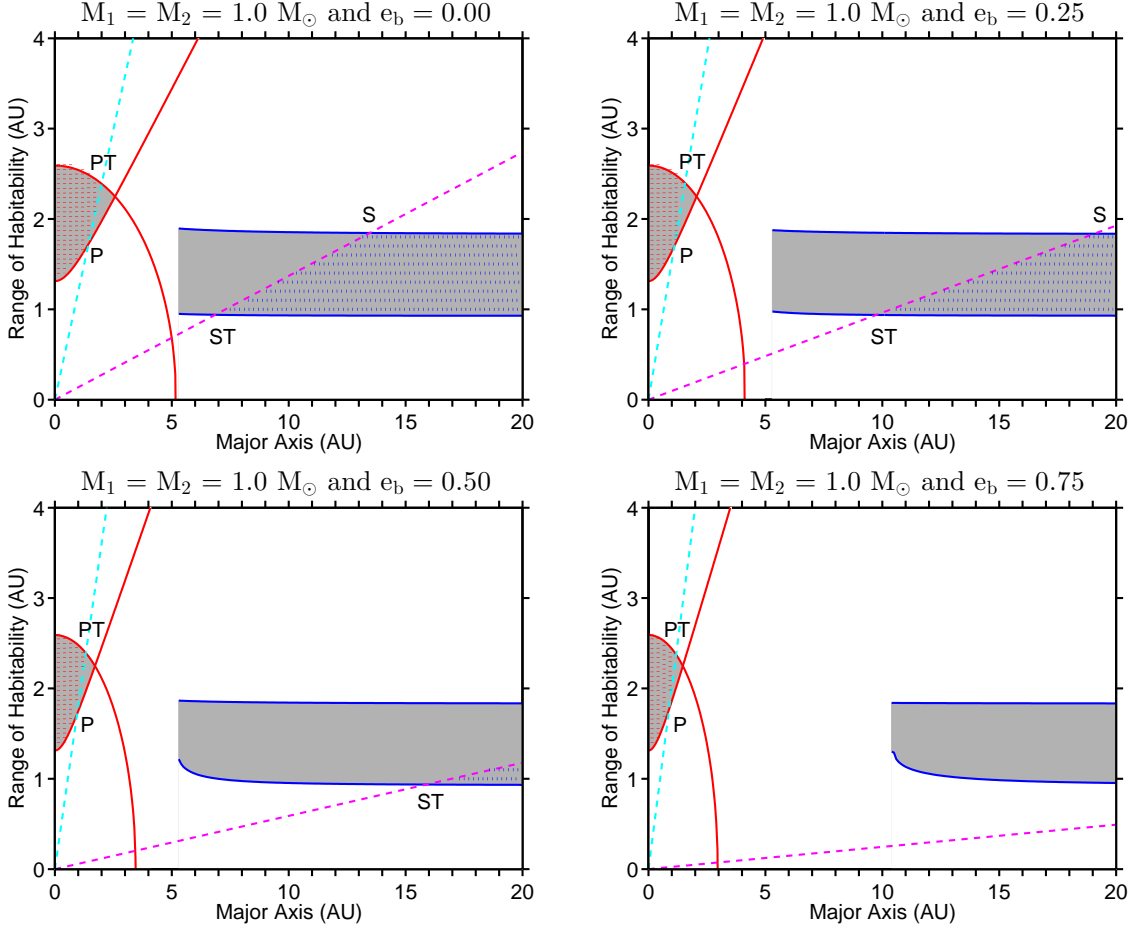


Fig. 6.— Range of habitability in equal-star binary systems with  $M_1 = M_2 = M_\odot$  for binary eccentricities of  $e_b = 0.00, 0.25, 0.50,$  and  $0.75,$  respectively. Results are obtained as a function of the binary major axis  $2a_b$  pertaining to the GHZ. The two red lines indicate the limits of the  $P$ -type RHZ (i.e.,  $\text{RHZ}_{\text{in}}$  and  $\text{RHZ}_{\text{out}}$ ), whereas the two blue lines indicate the limits of the  $S$ -type RHZ. The available  $S$ - and  $P$ -type RHZs are depicted as grayish areas. The cyan dashed line indicates the  $P$ -type orbital stability limit, whereas the violet dashed line indicates the  $S$ -type orbital stability limit. Note that the  $P$ -type orbital stability limit constitutes a lower limit, whereas the  $S$ -type orbital stability limit constitutes an upper limit; thus, the available ranges of habitability within the RHZs are indicated as red-hatched and blue-hatched areas, respectively. Hence,  $P$ -type habitability is attained in the range beneath the P intersection point,  $PT$ -type habitability between the intersection points P and PT,  $ST$ -type habitability between the intersection points ST and S, and  $S$ -type habitability beyond the S intersection point. No habitability is found between the intersection points PT and ST. For  $e_b = 0.50,$  the intersects of ST and S are given as 15.9 and 31.1 AU, whereas for  $e_b = 0.75,$  they are given as 38.0 and 74.5 AU, respectively.

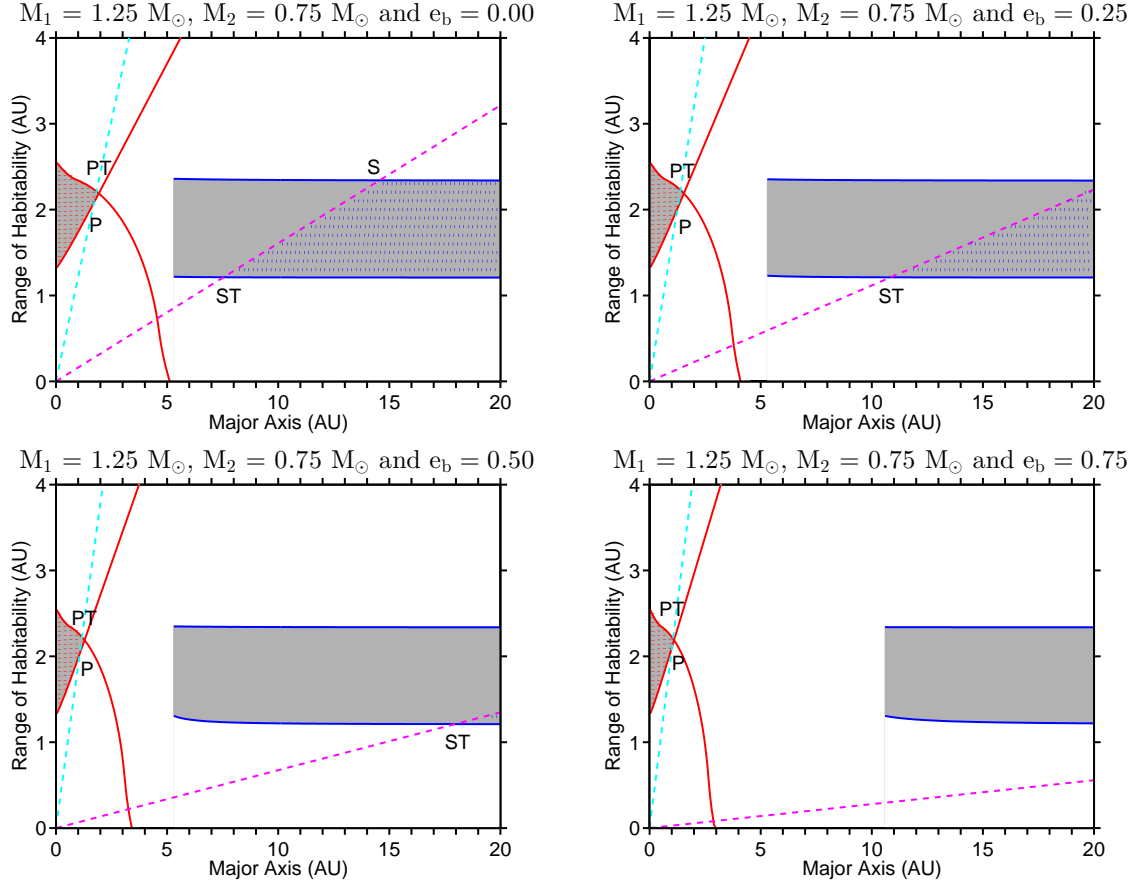


Fig. 7.— Same as Figure 6, but now for an unequal-star binary system with  $M_1 = 1.25 M_\odot$  and  $M_2 = 0.75 M_\odot$ . For  $e_b = 0.50$ , the intersects of ST and S are given as 18.2 and 35.1 AU, denoting the domain of *ST*-type habitability, whereas for  $e_b = 0.75$ , they are given as 43.9 and 84.9 AU, respectively.

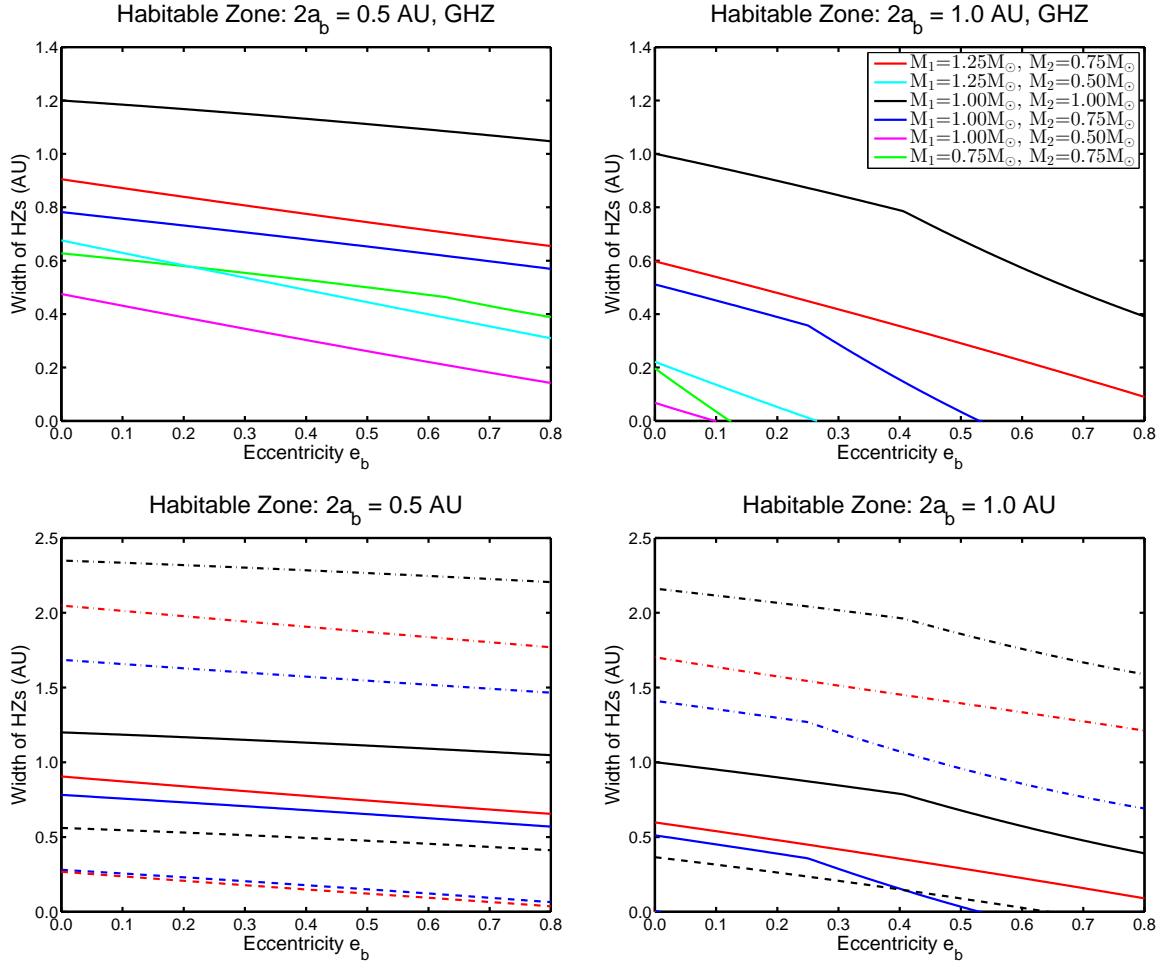


Fig. 8.— Widths of  $P/PT$ -type habitable zones of various binary systems for  $2a_b = 0.5$  AU (left column) and  $2a_b = 1.0$  AU (right column). The top row depicts results for the GHZ for six systems, whereas the bottom row depicts results for the EHZ (dash-dotted), GHZ (solid), and CHZ (dashed) for a selection of three systems (see top right subfigure for color code). The line explanations for the bottom row is given as part of Fig. 9 for stylistic reasons.



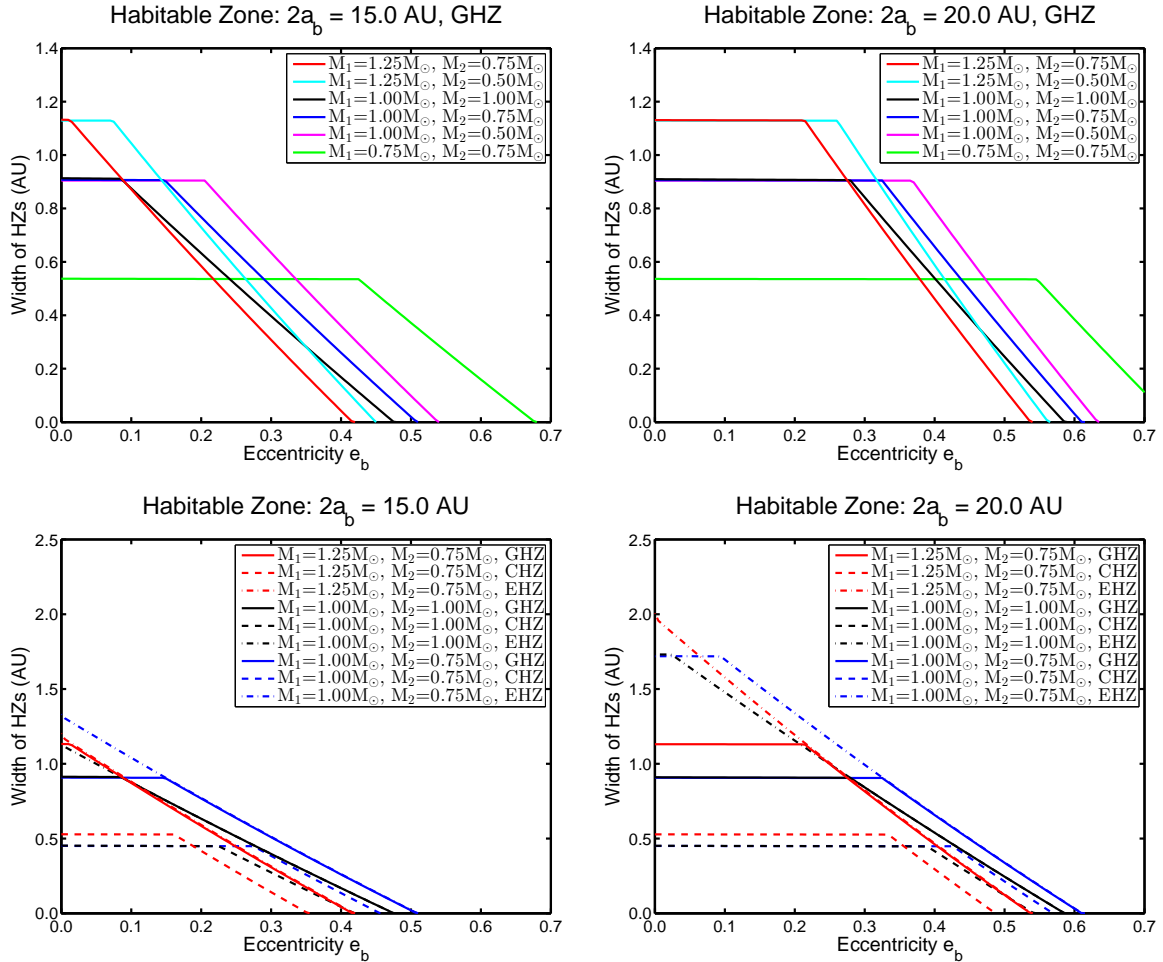


Fig. 9.— Widths of  $S/ST$ -type habitable zones of various binary systems for  $2a_b = 15.0$  AU (left column) and  $2a_b = 20.0$  AU (right column). The top row depicts results for the GHZ for six systems, whereas the bottom row depicts results for the EHZ (dash-dotted), GHZ (solid), and CHZ (dashed) for a selection of three systems.

Table 1. Stellar Parameters

Sp. Type	$T_{\text{eff}}$	$R_*$	$L_*$	$S_{\text{rel},*}$	$M_*$
...	(K)	( $R_{\odot}$ )	( $L_{\odot}$ )	...	( $M_{\odot}$ )
F0	7178	1.62	6.255	1.145	1.60
F2	6909	1.48	4.481	1.113	1.52
F5	6528	1.40	3.196	1.072	1.40
F8	6160	1.20	1.862	1.037	1.19
G0	5943	1.12	1.405	1.019	1.05
G2	5811	1.08	1.194	1.009	0.99
G5	5657	0.95	0.830	0.997	0.91
G8	5486	0.91	0.673	0.985	0.84
K0	5282	0.83	0.481	0.971	0.79
K2	5055	0.75	0.330	0.957	0.74
K5	4487	0.64	0.149	0.926	0.67
K8	4006	0.53	0.066	0.905	0.58
M0	3850	0.48	0.045	0.900	0.51

Note. — Adopted from Paper I.

Table 2. Definition of  $\tilde{a}_{\text{SP},\ell}$

$\ell$	$s_\ell$	$\tilde{a}_{\text{SP},\ell}$		HZ Limit
...	...	<i>S</i> -Type	<i>P</i> -Type	...
...	(AU)	(AU)	(AU)	...
1	0.84	$a_b(1 - e_b)$	$a_b(1 + e_b)$	GHZ / EHZ
2	0.95	$a_b(1 - e_b)$	$a_b(1 + e_b)$	CHZ
3	1.00	$a_b$	$a_b$	...
4	1.37	$a_b(1 + e_b)$	$a_b(1 + e_b)$	CHZ
5	1.67	$a_b(1 + e_b)$	$a_b(1 + e_b)$	GHZ
6	2.40	$a_b(1 + e_b)$	$a_b(1 + e_b)$	EHZ

Note. — The case of  $\ell = 3$  depicts an Earth-equivalent position denoting a planetary reference distance without the consideration of eccentricity.

Table 3. Orbital Stability Parameters Following HW99

Parameter	<i>S</i> -Type	<i>P</i> -Type
$\tilde{A}_0$	0.464	1.60
$\tilde{A}_1$	-0.380	4.12
$\tilde{A}_2$	0.0	-5.09
$\tilde{B}_0$	-0.631	5.10
$\tilde{B}_1$	0.586	-4.27
$\tilde{B}_2$	0.0	0.0
$\tilde{C}_0$	0.150	-2.22
$\tilde{C}_1$	-0.198	0.0
$\tilde{C}_2$	0.0	4.61

Table 4. RHZs of  $P$ -Type Orbits for  $M_1 = M_2 = 1.0 M_\odot$ , CHZ

$e_b$	$a_{\text{per}}$		$a_{\text{ap}}$		Orbit		$a_{\text{cr}}$	%RHZ	%HZ	Type
...	RHZ <sub>in</sub>	RHZ <sub>out</sub>	RHZ <sub>in</sub>	RHZ <sub>out</sub>	RHZ <sub>in</sub>	RHZ <sub>out</sub>	...	...	...	...
...	(AU)	(AU)	(AU)	(AU)	(AU)	(AU)	(AU)	...	...	...
Model: $2a_b = 0.50$ AU										
0.00	1.544	2.105	1.544	2.105	1.54	2.11	0.60	100	100	$P$
0.10	1.533	2.108	1.556	2.102	1.56	2.10	0.67	97	97	$P$
0.20	1.523	2.111	1.569	2.099	1.57	2.10	0.73	94	94	$P$
0.30	1.515	2.113	1.582	2.095	1.58	2.09	0.80	91	91	$P$
0.40	1.507	2.115	1.596	2.091	1.60	2.09	0.85	88	88	$P$
0.50	1.500	2.116	1.611	2.087	1.61	2.09	0.90	85	85	$P$
0.60	1.494	2.118	1.627	2.082	1.63	2.08	0.95	81	81	$P$
0.70	1.490	2.119	1.643	2.077	1.64	2.08	0.98	77	77	$P$
0.80	1.487	2.119	1.660	2.072	1.66	2.07	1.02	73	73	$P$
Model: $2a_b = 0.75$ AU										
0.00	1.611	2.087	1.611	2.087	1.61	2.09	0.90	100	100	$P$
0.10	1.589	2.093	1.635	2.080	1.64	2.08	1.00	94	94	$P$
0.20	1.569	2.099	1.660	2.072	1.66	2.07	1.10	87	87	$P$
0.30	1.550	2.104	1.686	2.063	1.69	2.06	1.19	79	79	$P$
0.40	1.533	2.108	1.713	2.054	1.71	2.05	1.28	72	72	$P$
0.50	1.519	2.112	1.742	2.044	1.74	2.04	1.35	64	64	$P$
0.60	1.507	2.115	1.771	2.033	1.77	2.03	1.42	55	55	$P$
0.70	1.497	2.117	1.800	2.022	1.80	2.02	1.48	47	47	$P$
0.80	1.490	2.119	1.831	2.010	1.83	2.01	1.53	38	38	$P$
Model: $2a_b = 1.0$ AU										
0.00	1.695	2.060	1.695	2.060	1.70	2.06	1.19	100	100	$P$
0.10	1.660	2.072	1.732	2.047	1.73	2.05	1.34	86	86	$P$
0.20	1.627	2.082	1.771	2.033	1.77	2.03	1.47	72	72	$P$
0.30	1.596	2.091	1.811	2.018	1.81	2.02	1.59	57	57	$P$
0.40	1.569	2.099	1.852	2.001	1.85	2.00	1.70	41	41	$P$
0.50	1.544	2.105	1.894	1.983	1.89	1.98	1.80	24	24	$P$
0.60	1.523	2.111	1.937	1.963	1.94	1.96	1.89	7	7	$P$
0.70	1.507	2.115	...	...	...	...	1.97	0	0	...
0.80	1.494	2.118	...	...	...	...	2.04	0	0	...

Note. — Here as well as in the subsequent Tables 5, 6, 7, 9, and 10, the data for  $a_{\text{per}}$  and  $a_{\text{ap}}$  are given in high precision for tutorial reasons.

Table 5. RHZs of  $P$ -Type Orbits for  $M_1 = M_2 = 1.0 M_\odot$ , GHz

$e_b$	$a_{\text{per}}$		$a_{\text{ap}}$		Orbit		$a_{\text{cr}}$	%RHZ	%HZ	Type
...	RHZ <sub>in</sub>	RHZ <sub>out</sub>	RHZ <sub>in</sub>	RHZ <sub>out</sub>	RHZ <sub>in</sub>	RHZ <sub>out</sub>	...	...	...	...
...	(AU)	(AU)	(AU)	(AU)	(AU)	(AU)	(AU)	...	...	...
Model: $2a_b = 0.50$ AU										
0.00	1.379	2.579	1.379	2.579	1.38	2.58	0.60	100	100	$P$
0.10	1.367	2.581	1.392	2.576	1.39	2.58	0.67	99	99	$P$
0.20	1.356	2.583	1.405	2.573	1.41	2.57	0.73	97	97	$P$
0.30	1.346	2.585	1.420	2.570	1.42	2.57	0.80	96	96	$P$
0.40	1.337	2.586	1.436	2.567	1.44	2.57	0.85	94	94	$P$
0.50	1.329	2.588	1.452	2.563	1.45	2.56	0.90	93	93	$P$
0.60	1.323	2.589	1.469	2.560	1.47	2.56	0.95	91	91	$P$
0.70	1.318	2.590	1.486	2.556	1.49	2.56	0.98	89	89	$P$
0.80	1.315	2.590	1.504	2.551	1.50	2.55	1.02	87	87	$P$
Model: $2a_b = 0.75$ AU										
0.00	1.452	2.563	1.452	2.563	1.45	2.56	0.90	100	100	$P$
0.10	1.428	2.569	1.477	2.558	1.48	2.56	1.00	97	97	$P$
0.20	1.405	2.573	1.504	2.551	1.50	2.55	1.10	94	94	$P$
0.30	1.385	2.577	1.532	2.544	1.53	2.54	1.19	91	91	$P$
0.40	1.367	2.581	1.561	2.537	1.56	2.54	1.28	88	88	$P$
0.50	1.350	2.584	1.590	2.529	1.59	2.53	1.35	84	84	$P$
0.60	1.337	2.586	1.621	2.520	1.62	2.52	1.42	81	81	$P$
0.70	1.326	2.588	1.652	2.511	1.65	2.51	1.48	77	77	$P$
0.80	1.318	2.590	1.684	2.501	1.68	2.50	1.53	74	74	$P$
Model: $2a_b = 1.0$ AU										
0.00	1.541	2.542	1.541	2.542	1.54	2.54	1.19	100	100	$P$
0.10	1.504	2.551	1.580	2.532	1.58	2.53	1.34	95	95	$P$
0.20	1.469	2.560	1.621	2.520	1.62	2.52	1.47	90	90	$P$
0.30	1.436	2.567	1.663	2.508	1.66	2.51	1.59	84	84	$P$
0.40	1.405	2.573	1.705	2.494	1.71	2.49	1.70	79	79	$P$
0.50	1.379	2.579	1.749	2.480	1.75	2.48	1.80	73	68	$PT$
0.60	1.356	2.583	1.793	2.464	1.79	2.46	1.89	67	57	$PT$
0.70	1.337	2.586	1.838	2.447	1.84	2.45	1.97	61	48	$PT$
0.80	1.323	2.589	1.884	2.429	1.88	2.43	2.04	55	39	$PT$

Table 6. RHZs of  $P$ -Type Orbits for  $M_1 = 1.25 M_\odot$ ,  $M_2 = 0.75 M_\odot$ , CHZ

$e_b$	$a_{\text{per}}$		$a_{\text{ap}}$		Orbit		$a_{\text{cr}}$	%RHZ	%HZ	Type
	RHZ <sub>in</sub>	RHZ <sub>out</sub>	RHZ <sub>in</sub>	RHZ <sub>out</sub>	RHZ <sub>in</sub>	RHZ <sub>out</sub>				
...	(AU)	(AU)	(AU)	(AU)	(AU)	(AU)	(AU)	...	...	...
Model: $2a_b = 0.50$ AU										
0.00	1.685	1.953	1.685	1.953	1.68	1.95	0.61	100	100	$P$
0.10	1.663	1.963	1.706	1.944	1.71	1.94	0.69	89	89	$P$
0.20	1.642	1.973	1.728	1.936	1.73	1.94	0.76	77	77	$P$
0.30	1.621	1.985	1.751	1.929	1.75	1.93	0.83	66	66	$P$
0.40	1.600	1.997	1.773	1.922	1.77	1.92	0.89	56	56	$P$
0.50	1.580	2.010	1.796	1.917	1.80	1.92	0.94	45	45	$P$
0.60	1.560	2.024	1.818	1.912	1.82	1.91	0.99	35	35	$P$
0.70	1.541	2.038	1.841	1.907	1.84	1.91	1.02	24	24	$P$
0.80	1.522	2.053	1.864	1.901	1.86	1.90	1.05	14	14	$P$
Model: $2a_b = 0.75$ AU										
0.00	1.796	1.917	1.796	1.917	1.80	1.92	0.91	100	100	$P$
0.10	1.762	1.925	1.830	1.909	1.83	1.91	1.04	66	66	$P$
0.20	1.728	1.936	1.864	1.901	1.86	1.90	1.15	30	30	$P$
0.30	1.695	1.948	...	...	...	...	1.25	0	0	...
0.40	1.663	1.963	...	...	...	...	1.34	0	0	...
0.50	1.631	1.979	...	...	...	...	1.41	0	0	...
0.60	1.600	1.997	...	...	...	...	1.48	0	0	...
0.70	1.570	2.017	...	...	...	...	1.54	0	0	...
0.80	1.541	2.038	...	...	...	...	1.58	0	0	...

Note. — Regarding the model  $2a_b = 1.0$  AU, the values for RHZ<sub>in</sub> and RHZ<sub>out</sub> are undefined as no HZs are identified for any of the models.

Table 7. RHZs of  $P$ -Type Orbits for  $M_1 = 1.25 M_\odot$ ,  $M_2 = 0.75 M_\odot$ , GHZ

$e_b$	$a_{\text{per}}$		$a_{\text{ap}}$		Orbit		$a_{\text{cr}}$	%RHZ	%HZ	Type
...	RHZ <sub>in</sub>	RHZ <sub>out</sub>	RHZ <sub>in</sub>	RHZ <sub>out</sub>	RHZ <sub>in</sub>	RHZ <sub>out</sub>	...	...	...	...
...	(AU)	(AU)	(AU)	(AU)	(AU)	(AU)	(AU)	...	...	...
Model: $2a_b = 0.50$ AU										
0.00	1.512	2.417	1.512	2.417	1.51	2.42	0.61	100	100	$P$
0.10	1.490	2.429	1.534	2.406	1.53	2.41	0.69	96	96	$P$
0.20	1.469	2.441	1.557	2.396	1.56	2.40	0.76	93	93	$P$
0.30	1.448	2.454	1.579	2.386	1.58	2.39	0.83	89	89	$P$
0.40	1.427	2.468	1.602	2.377	1.60	2.38	0.89	86	86	$P$
0.50	1.406	2.482	1.625	2.369	1.62	2.37	0.94	82	82	$P$
0.60	1.386	2.497	1.648	2.361	1.65	2.36	0.99	79	79	$P$
0.70	1.367	2.512	1.671	2.355	1.67	2.35	1.02	76	76	$P$
0.80	1.348	2.527	1.694	2.349	1.69	2.35	1.05	72	72	$P$
Model: $2a_b = 0.75$ AU										
0.00	1.625	2.369	1.625	2.369	1.62	2.37	0.91	100	100	$P$
0.10	1.590	2.382	1.659	2.358	1.66	2.36	1.04	94	94	$P$
0.20	1.557	2.396	1.694	2.349	1.69	2.35	1.15	88	88	$P$
0.30	1.523	2.412	1.729	2.341	1.73	2.34	1.25	82	82	$P$
0.40	1.490	2.429	1.764	2.333	1.76	2.33	1.34	76	76	$P$
0.50	1.458	2.448	1.800	2.324	1.80	2.32	1.42	70	70	$P$
0.60	1.427	2.468	1.836	2.315	1.84	2.31	1.48	64	64	$P$
0.70	1.396	2.489	1.872	2.305	1.87	2.30	1.54	58	58	$P$
0.80	1.367	2.512	1.908	2.294	1.91	2.29	1.58	52	52	$P$
Model: $2a_b = 1.0$ AU										
0.00	1.741	2.338	1.741	2.338	1.74	2.34	1.21	100	100	$P$
0.10	1.694	2.349	1.788	2.327	1.79	2.33	1.38	90	90	$P$
0.20	1.648	2.361	1.836	2.315	1.84	2.31	1.53	80	80	$P$
0.30	1.602	2.377	1.883	2.301	1.88	2.30	1.66	70	70	$P$
0.40	1.557	2.396	1.932	2.287	1.93	2.29	1.78	59	59	$P$
0.50	1.512	2.417	1.980	2.271	1.98	2.27	1.89	49	49	$P$
0.60	1.469	2.441	2.028	2.254	2.03	2.25	1.98	38	38	$P$
0.70	1.427	2.468	2.077	2.235	2.08	2.24	2.05	26	26	$P$
0.80	1.386	2.497	2.126	2.216	2.13	2.22	2.11	15	15	$P$



Table 8. Critical Values of  $e_b$  for Models of  $P/PT$ -Type Habitability

Binary Major Axis ( $2a_b$ )	0.5 AU		1.0 AU	
Model	CHZ	GHZ	CHZ	GHZ
$M_1 = 1.25 M_\odot, M_2 = 1.25 M_\odot$	†	†	†	†
$M_1 = 1.25 M_\odot, M_2 = 1.00 M_\odot$	†	†	0.64	†
$M_1 = 1.25 M_\odot, M_2 = 0.75 M_\odot$	†	†	...	†
$M_1 = 1.25 M_\odot, M_2 = 0.50 M_\odot$	0.16	†	...	0.26
$M_1 = 1.00 M_\odot, M_2 = 1.00 M_\odot$	†	†	0.64	†
$M_1 = 1.00 M_\odot, M_2 = 0.75 M_\odot$	†	†	0.006	0.53
$M_1 = 1.00 M_\odot, M_2 = 0.50 M_\odot$	0.05	†	...	0.10
$M_1 = 0.75 M_\odot, M_2 = 0.75 M_\odot$	†	†	...	0.12
$M_1 = 0.75 M_\odot, M_2 = 0.50 M_\odot$	...	0.53	...	...
$M_1 = 0.50 M_\odot, M_2 = 0.50 M_\odot$	...	...	...	...

Note. — (†) means that the critical value of  $e_b$  is larger than 0.80; it could not be determined owing to the limitations of the work by HW99. Dots indicate that there is no solution.

Table 9. RHZs of  $S$ -Type Orbits for  $M_1 = M_2 = 1.0 M_\odot$

$e_b$	$a_{\text{per}}$		$a_{\text{ap}}$		Orbit		$a_{\text{cr}}$	%RHZ	%HZ	Type
...	RHZ <sub>in</sub>	RHZ <sub>out</sub>	RHZ <sub>in</sub>	RHZ <sub>out</sub>	RHZ <sub>in</sub>	RHZ <sub>out</sub>	...	...	...	...
...	(AU)	(AU)	(AU)	(AU)	(AU)	(AU)	(AU)	...	...	...
Model: $2a_b = 20.0$ AU, CHZ										
0.00	1.0513	1.5027	1.0513	1.5027	1.05	1.50	2.74	100.0	100.0	$S$
0.10	1.0517	1.5035	1.0510	1.5021	1.05	1.50	2.41	99.8	99.8	$S$
0.20	1.0523	1.5046	1.0508	1.5017	1.05	1.50	2.08	99.5	99.5	$S$
0.30	1.0531	1.5061	1.0506	1.5013	1.05	1.50	1.77	99.3	99.3	$S$
0.40	1.0545	1.5084	1.0505	1.5010	1.05	1.50	1.47	98.9	91.9	$ST$
0.50	1.0570	1.5120	1.0504	1.5008	1.06	1.50	1.18	98.3	26.7	$ST$
0.60	1.0619	1.5180	1.0503	1.5006	1.06	1.50	0.90	97.2	0.0	...
0.70	1.0743	1.5297	1.0502	1.5004	1.07	1.50	0.62	94.4	0.0	...
0.80	1.1277	1.5568	1.0501	1.5003	1.13	1.50	0.36	82.5	0.0	...
Model: $2a_b = 20.0$ AU, GHZ										
0.00	0.9287	1.8384	0.9287	1.8384	0.93	1.84	2.74	100.0	100.0	$S$
0.10	0.9290	1.8398	0.9285	1.8373	0.93	1.84	2.41	99.9	99.9	$S$
0.20	0.9294	1.8416	0.9284	1.8365	0.93	1.84	2.08	99.7	99.7	$S$
0.30	0.9300	1.8443	0.9283	1.8359	0.93	1.84	1.77	99.6	92.6	$ST$
0.40	0.9309	1.8481	0.9282	1.8354	0.93	1.84	1.47	99.4	59.2	$ST$
0.50	0.9325	1.8542	0.9281	1.8349	0.93	1.84	1.18	99.2	26.9	$ST$
0.60	0.9357	1.8643	0.9281	1.8346	0.94	1.83	0.90	98.8	0.0	...
0.70	0.9437	1.8834	0.9280	1.8343	0.94	1.83	0.62	97.9	0.0	...
0.80	0.9746	1.9262	0.9280	1.8340	0.97	1.83	0.36	94.5	0.0	...

Table 10. RHZs of *S*-Type Orbits for  $M_1 = 1.25 M_\odot$ ,  $M_2 = 0.75 M_\odot$

$e_b$	$a_{\text{per}}$		$a_{\text{ap}}$		Orbit		$a_{\text{cr}}$	%RHZ	%HZ	Type
...	RHZ <sub>in</sub>	RHZ <sub>out</sub>	RHZ <sub>in</sub>	RHZ <sub>out</sub>	RHZ <sub>in</sub>	RHZ <sub>out</sub>	...	...	...	...
...	(AU)	(AU)	(AU)	(AU)	(AU)	(AU)	(AU)	...	...	...
Model: $2a_b = 20.0$ AU, CHZ										
0.00	1.3703	1.8981	1.3703	1.8981	1.37	1.90	3.22	100.0	100.0	<i>S</i>
0.10	1.3705	1.8984	1.3702	1.8979	1.37	1.90	2.77	99.9	99.9	<i>S</i>
0.20	1.3707	1.8988	1.3701	1.8977	1.37	1.90	2.39	99.8	99.8	<i>S</i>
0.30	1.3711	1.8994	1.3700	1.8975	1.37	1.90	2.02	99.7	99.7	<i>S</i>
0.40	1.3717	1.9003	1.3699	1.8974	1.37	1.90	1.67	99.6	55.8	<i>ST</i>
0.50	1.3727	1.9017	1.3699	1.8973	1.37	1.90	1.33	99.4	0.0	...
0.60	1.3749	1.9039	1.3699	1.8972	1.37	1.90	1.01	99.0	0.0	...
0.70	1.3804	1.9081	1.3699	1.8972	1.38	1.90	0.70	97.9	0.0	...
0.80	1.4046	...	1.3699	1.8971	1.40	1.90	0.40	93.3	0.0	...
Model: $2a_b = 20.0$ AU, GHZ										
0.00	1.2087	2.3394	1.2087	2.3394	1.21	2.34	3.22	100.00	100.00	<i>S</i>
0.10	1.2088	2.3399	1.2086	2.3390	1.21	2.34	2.77	99.95	99.95	<i>S</i>
0.20	1.2090	2.3407	1.2085	2.3387	1.21	2.34	2.39	99.91	99.91	<i>S</i>
0.30	1.2092	2.3417	1.2085	2.3384	1.21	2.34	2.02	99.87	72.1	<i>ST</i>
0.40	1.2096	2.3431	1.2085	2.3382	1.21	2.34	1.67	99.82	40.8	<i>ST</i>
0.50	1.2103	2.3453	1.2084	2.3381	1.21	2.34	1.33	99.7	10.8	<i>ST</i>
0.60	1.2117	2.3489	1.2084	2.3379	1.21	2.34	1.01	99.6	0.0	...
0.70	1.2152	2.3554	1.2084	2.3378	1.22	2.34	0.70	99.3	0.0	...
0.80	1.2293	...	1.2084	2.3377	1.23	2.34	0.42	98.0	0.0	...

Table 11. Critical Values of  $e_b$  for Models of  $S/ST$ -Type Habitability

Binary Major Axis ( $2a_b$ )	15.0 AU		20.0 AU	
Model	CHZ	GHZ	CHZ	GHZ
$M_1 = 1.25 M_\odot, M_2 = 1.25 M_\odot$	0.28	0.35	0.43	0.49
$M_1 = 1.25 M_\odot, M_2 = 1.00 M_\odot$	0.31	0.38	0.46	0.51
$M_1 = 1.25 M_\odot, M_2 = 0.75 M_\odot$	0.35	0.42	0.49	0.54
$M_1 = 1.25 M_\odot, M_2 = 0.50 M_\odot$	0.39	0.45	0.51	0.56
$M_1 = 1.00 M_\odot, M_2 = 1.00 M_\odot$	0.42	0.48	0.54	0.59
$M_1 = 1.00 M_\odot, M_2 = 0.75 M_\odot$	0.46	0.51	0.57	0.61
$M_1 = 1.00 M_\odot, M_2 = 0.50 M_\odot$	0.49	0.54	0.59	0.63
$M_1 = 0.75 M_\odot, M_2 = 0.75 M_\odot$	0.64	0.68	0.72	0.74
$M_1 = 0.75 M_\odot, M_2 = 0.50 M_\odot$	0.67	0.70	0.73	0.76
$M_1 = 0.50 M_\odot, M_2 = 0.50 M_\odot$	†	†	†	†

Note. — (†) means that the critical value of  $e_b$  is larger than 0.80; it could not be determined owing to the limitations of the work by HW99.